Dunning + Japan) —

DR 637

Dietz

ORNL-4907
(ENDF-203)

# $^{54}$Fe NEUTRON ELASTIC AND INELASTIC SCATTERING CROSS SECTIONS FROM 5.50 TO 8.50 MeV


W. E. Kinney
F. G. Perey


MASTER

BLANK PAGE

Printed in the United States of America. Available from
National Technical Information Service
U.S. Department of Commerce
5285 Port Royal Road, Springfield, Virginia 22151
Price: Printed Copy $4.00; Microfiche $0.95

ORNL-4907
UC-79d
(ENDF-203)

Contract No. W-7405-eng-26

Neutron Physics Division

# $^{54}$Fe NEUTRON ELASTIC AND INELASTIC SCATTERING CROSS SECTIONS FROM 5.50 TO 8.50 MeV

W. E. Kinney and F. G. Perey

FEBRUARY 1974



OAK RIDGE NATIONAL LABORATORY
Oak Ridge, Tennessee 37830
operated by
UNION CARBIDE CORPORATION
for the
U.S. ATOMIC ENERGY COMMISSION

# CONTENTS

## $^{54}$Fe NEUTRON ELASTIC AND INELASTIC SCATTERING

## CROSS SECTIONS FROM 5.50 TO 8.50 MeV

W. E. Kinney and F. G. Perey


## ABSTRACT

Measured $^{54}$Fe neutron elastic scattering cross sections and cross sections for inelastic scattering to 7 discrete levels or groups of levels in $^{54}$Fe in the incident neutron energy range from 5.50 to 8.50 MeV are presented. The elastic data are in good agreement with our previously reported natural iron results. Inelastic scattering to the 1.409 MeV level shows evidence of direct reaction contributions at the higher incident neutron energies. ENDF/B III MAT 1180 natural iron cross sections for inelastic scattering to the 1.409 MeV level in $^{54}$Fe are higher by a factor of 2 than our data. Cross sections for inelastic scattering to levels in the residual nucleus of excitation energy greater than 4.29 MeV are presented as continuum cross sections. It is found that an evaporation model of continuum inelastic scattering is adequate above 6.2 MeV excitation energy but is questionable in describing inelastic scattering to lower-lying levels.


## INTRODUCTION

The data reported here are the results of one of a series of experiments to measure neutron elastic and inelastic scattering cross sections at the ORNL Van de Graaffs. Reports in the series are listed in Reference 1. This report presents measured neutron elastic and inelastic scattering cross sections for $^{54}$Fe from 5.50 to 8.50 MeV. To assist in the evaluation of the data, the data acquisition and reduction techniques are first briefly discussed. For the purposes of discussion the data are presented in graphical form and compared with our previous results for natural iron[1] and with ENDF/B III (Evaluated Neutron Data File B, Version III) MAT 1180. Tables of numerical values of the elastic scattering cross sections and cross sections for inelastic scattering to discrete levels in the residual nucleus are given in an appendix.

## DATA ACQUISITION

The data were obtained with conventional time-of-flight techniques. Pulsed (2 MHz), bunched (approximately 1.5 nsec full width at half maximum, FWHM) deuterons accelerated by the ORNL Van de Graaffs interacted with deuterium in a gas cell to produce neutrons by the D(d,n)$^3$He reaction. The gas cells, of length 1 and 2 cm, were operated at pressures of approximately 1.5 atm and gave neutron energy resolutions of the order of ±60 keV.

The neutrons were scattered from a solid right circular cylindrical sample of $^{54}$Fe

(99.9% purity), 2.00 cm diameter, 2.00 cm high of mass 48.36 gm and placed approximately 10 cm from the gas cells when the detector angles were greater than 25 degrees. For smaller detector angles the cell-to-sample distance had to be increased to 33 cm in order to shield the detectors from neutrons coming directly from the gas cells.

The scattered neutrons were detected by 12.5 cm diameter NE-213 liquid scintillators optically coupled to XP-1040 photomultipliers. The scintillators were 2.5 cm thick. Data were taken with three detectors simultaneously. Flight paths were approximately 5 m with the detector angles ranging from 15 to 140 degrees. The gas cell neutron production was monitored by a time-of-flight system which used a 5 cm diameter by 2.5 cm thick NE-213 scintillator viewed by a 56-AVP photomultiplier placed about 4 m from the cell at an angle of 55 degrees with the incident deuteron beam.

For each event a PDP-7 computer was given the flight time of a detected recoil proton event with reference to a beam pulse signal, the pulse height of the recoil proton event, and identification of the detector. The electronic equipment for supplying this information to the computer consisted, for the most part, of standard commercial components. The electronic bias was set at approximately 700 keV neutron energy to ensure good pulse shape discrimination against gamma-rays at all energies.

The detector efficiencies were measured by (n,p) scattering from a 6 mm diameter polyethylene sample and by detecting source D(d,n)$^3$He neutrons at 0 degrees[2]. Both interactions gave results which agreed with each other and which yielded efficiency versus energy curves that compared well with calculations[3].

## DATA REDUCTION

Central to the data reduction process was the use of a light pen with the PDP-7 computer oscilloscope display programs to extract peak areas from spectra. The light pen made a comparatively easy job of estimating errors in the cross section caused by extreme but possible peak shapes.

The reduction process started by normalizing a sample-out to a sample-in time-of-flight spectrum by the ratio of their monitor neutron peak areas, subtracting the sample-out spectrum, and transforming the difference spectrum into a spectrum of center-of-mass cross section versus excitation energy. This transformation allowed ready comparison of spectra taken at different angles and incident neutron energies by removing kinematic effects. It also made all single peaks have approximately the same shape and width regardless of excitation energy (in a time-of-flight spectrum, single peaks broaden with increasing flight time). A spectrum of the variance based on the counting statistics of the initial data was also computed. Figure 1 shows a typical time-of-flight spectrum and its transformed energy spectrum.

The transformed spectra were read into the PDP-7 computer and the peak stripping was done with the aid of the light pen. A peak was stripped by drawing a background beneath it, subtracting the background, and calculating the area, centroid, and FWHM of the difference. The variance spectrum was used to compute a counting statistics variance corresponding to the stripped peak. Peak stripping errors due to uncertainties in the residual background under the peaks or to the tails of imperfectly resolved nearby peaks

ORNL-DWG 73-7298

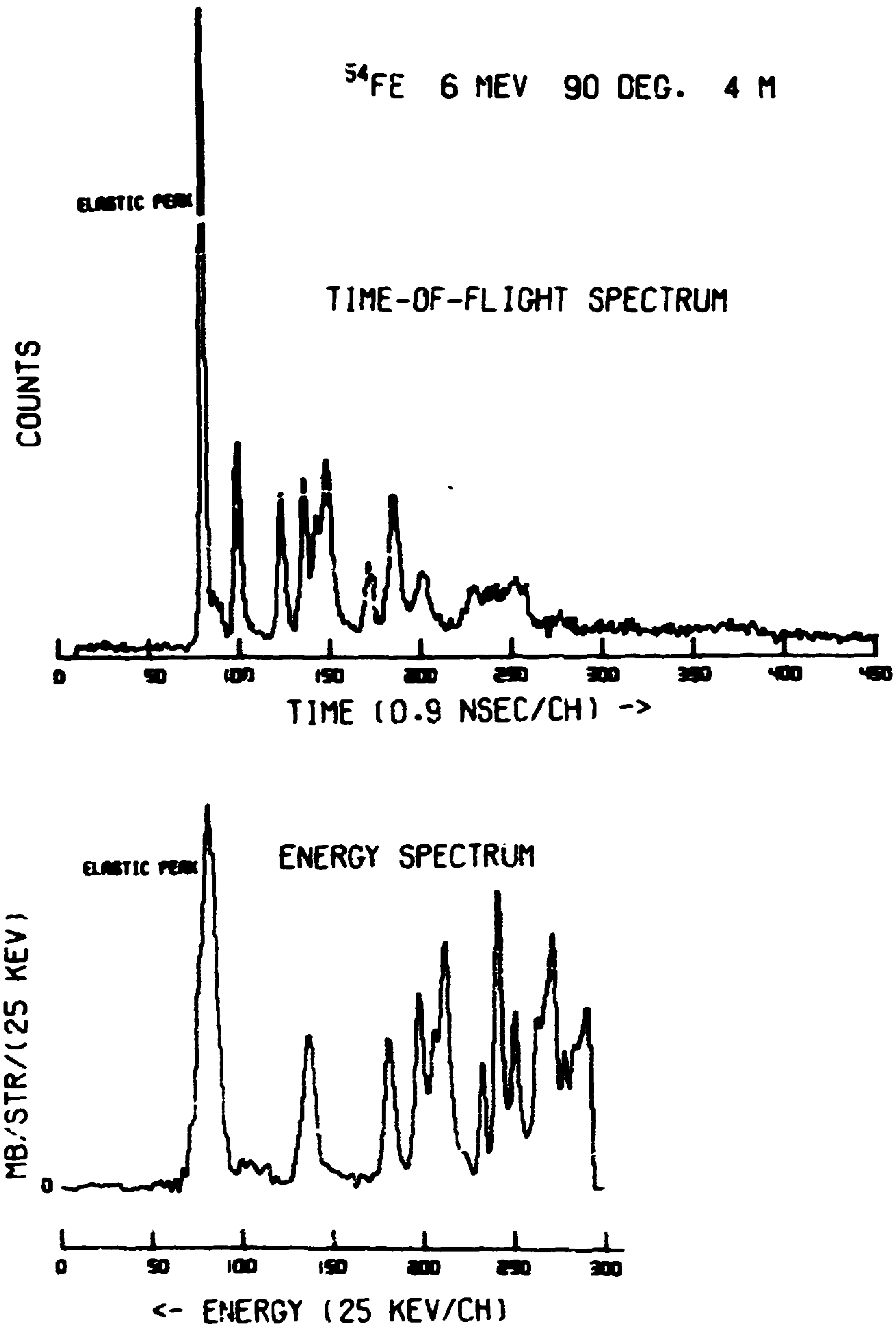


Fig. 1. A typical time-of-flight spectrum for $^{54}$Fe with its transformed energy spectrum. The data were taken at 6.0 MeV incident neutron energy at 90 degrees with a 4 m flight path. The sample-out spectrum has not been subtracted from the time-of-flight spectrum. Note that the energy spectrum has been offset to allow negative excursions due to statistics in the subtraction of the sample-out. The energy spectrum terminates at approximately 1 MeV scattered neutron energy - very nearly channel 350 in the time-of-flight spectrum. The large peaks to the left are the elastic peaks.

could be included with the other errors by stripping the peaks several times corresponding to high, low, and best estimates of this background. Although somewhat subjective, the low and high estimates of the cross sections were identified with 95% confidence limits; these, together with the best estimate, defined upper and lower errors due to stripping. When a spectrum was completely stripped, the output information was written on magnetic tape for additional processing by a large computer.

Finite sample corrections were performed according to semianalytic recipes whose constants were obtained from fits to Monte Carlo results[4]. The corrections were typically 5% at forward angles, 30% in the first minimum and 10 - 20% on the second maximum.

The final error analysis included uncertainties in the geometrical parameters (scatterer size, gas cell-to-scatterer distance, flight paths, etc.) and uncertainties in the finite sample corrections.

The measured differential elastic scattering cross sections were fitted by least squares to a Legendre series:

$$\sigma(\mu = \cos\theta) = \Sigma[(2k+1)/2)]a_k P_k(\mu)$$

the points being weighted by the inverse of their variances which were computed by squaring the average of the upper and lower uncertainties. The common 7% uncertainty in absolute normalization was not included in the variances for the fitting. In order to prevent the fit from giving totally unrealistic values outside the angular range of our measurements, we resorted to the inelegant but workable process of adding three points equally spaced in angle between the largest angle of measurement and 175 degrees. The differential cross sections at the added points were chosen to approximate the diffraction pattern at large angles, but were assigned 50% errors.

## RESULTS

### *Elastic Scattering Differential Cross Sections*

Our differential elastic scattering cross sections for $^{54}Fe$ are shown in Figure 2 with Legendre least squares fits to the data. Wick's Limit is shown and was used in the fitting.

Our $^{54}Fe$ differential elastic scattering cross sections are compared with our previously reported natural iron data[1] in Figure 3. The $^{54}Fe$ 5.50 MeV data are compared with natural iron results which were measured at 5.44 ± 0.17 MeV and at 5.56 ± 0.04 MeV.

These data generally agree within experimental uncertainties at angles less than 50 deg. The 5.44 MeV natural iron data seems to indicate the first minimum falling at a somewhat smaller angle than do the $^{54}Fe$ and natural iron 5.56 MeV data, if the low point in the latter data set is ignored. There is some structure in the total cross section at this energy[5] so that perhaps the different resolutions could account for the difference. More likely, however, the two low natural iron points around 60 deg. should be ignored and more weight given to the $^{54}Fe$ results since they are considerably more recent, these natural iron data being the very first resulting from our neutron elastic and inelastic scattering cross section measurement program[1]. The data from 6.53 to 7.54 MeV appear to be consistent in shape while the $^{54}Fe$ data at 8.50 MeV agrees within experimental uncertainties with the natural iron data which was measured at 8.56 ± 0.05 MeV.

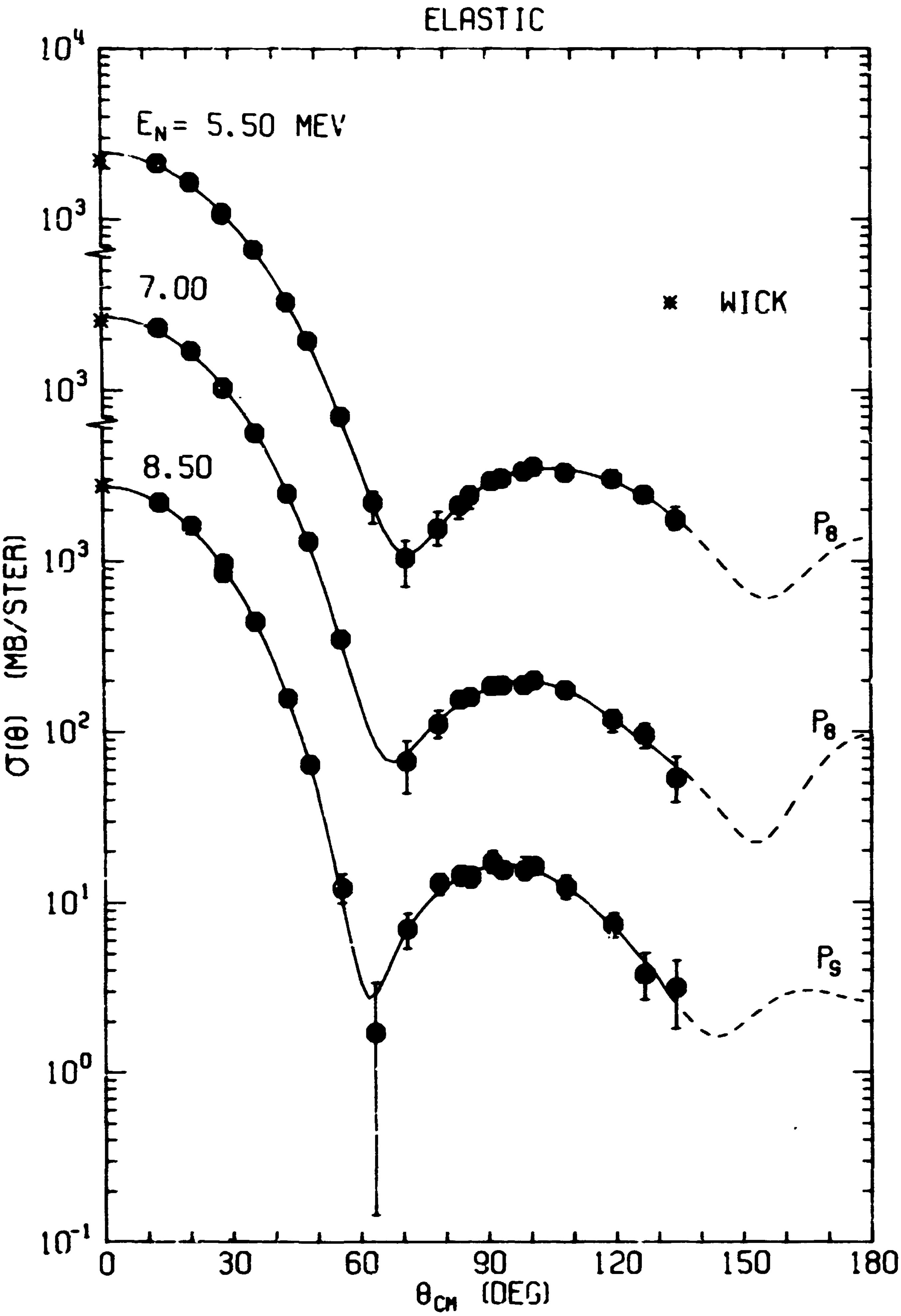


Fig. 2. Our $^{54}$Fe neutron differential elastic center-of-mass cross sections with Legendre fits to the data. WICK indicates Wick's Limit which was used in the fitting. The 7% uncertainty in absolute normalization common to all points is not included in the error bars.

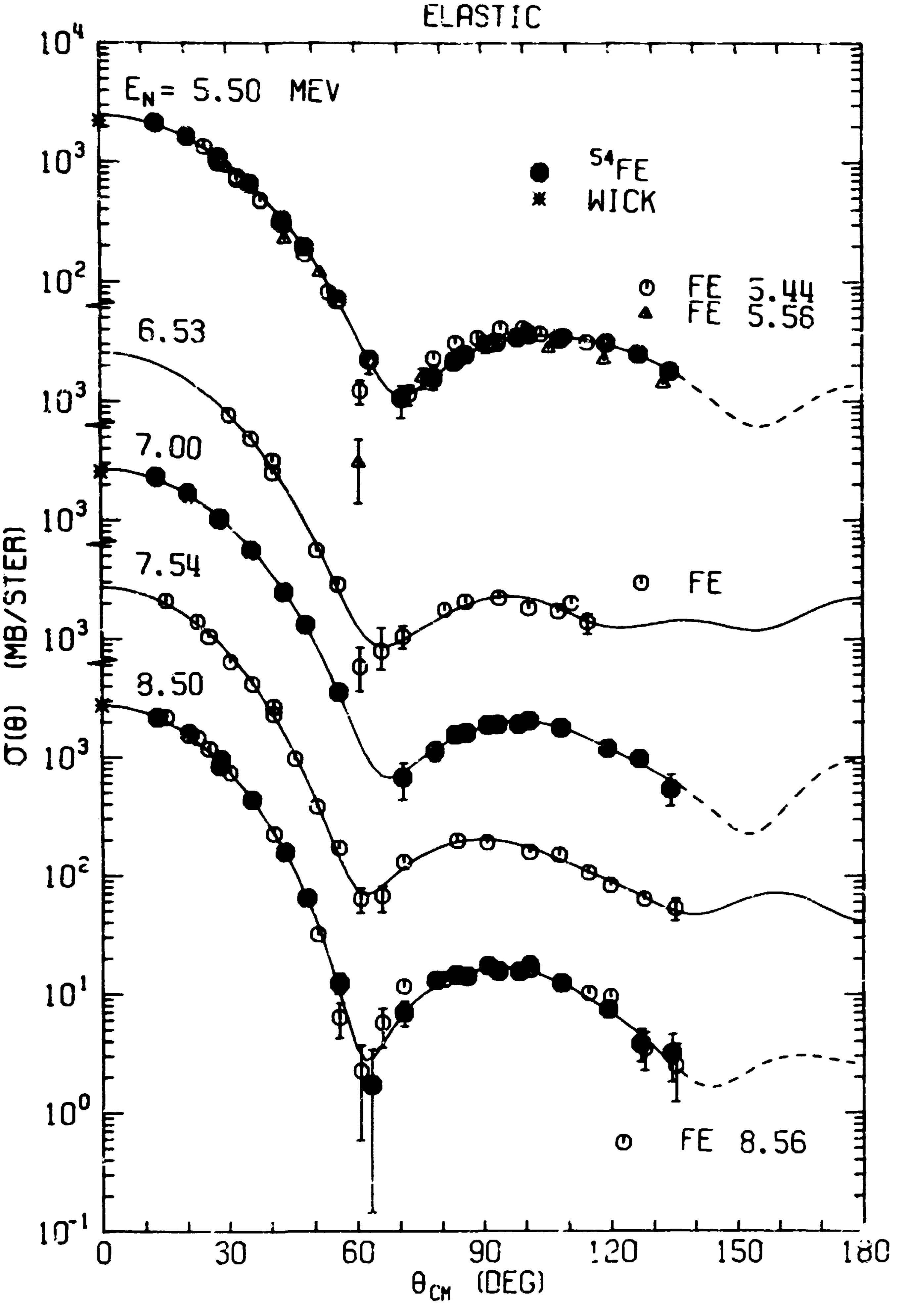


Fig. 3. A comparison of our $^{54}$Fe neutron differential elastic center-of-mass cross sections with our previously reported natural iron results. WICK indicates Wick's Limit. The 7% uncertainty in absolute normalization common to all points is not included in the error bars.

*Inelastic Scattering Differential Cross Sections*

Our differential cross sections for inelastic scattering to resolvable discrete levels or groups of levels in $^{54}$Fe are shown in Figures 4 through 7. The angular distribution of neutrons inelastically scattered to the $2^+$ 1.409 MeV level shown in Figure 4 might be expected to, and indeed does, show some asymmetry about 90 deg. due to the effect of direct interactions. ENDF/B III MAT 1180 assumes an isotropic angular distribution for inelastic scattering to this level.

The angular distributions of neutrons inelastically scattered to the other levels or groups of levels are isotropic within the experimental uncertainties.

*Excitation Functions*

Our angle-integrated differential cross sections for $^{54}$Fe as a function of incident neutron energy are shown in Figures 8 and 9. In Figure 8 we compare the $^{54}$Fe angle-integrated differential elastic scattering cross sections with previously reported values for natural iron[1] and with the ENDF/B III MAT 1180 curve for inelastic scattering to the 1.409 MeV level but with its values divided by the natural abundance of $^{54}$Fe for the comparison.

The elastic $^{54}$Fe and natural iron results are in good agreement while the ENDF/B III MAT 1180 curve is roughly a factor of 2 higher than our data.

The inelastic scattering cross sections to the higher-lying levels decrease with increasing energy as competition from additional exit channels increases.

As with $^{56}$Fe, neutron elastic and inelastic scattering on $^{54}$Fe should be quite amenable to optical model, Hauser-Feshbach, and distorted-wave-Born-approximation analysis.

*Inelastic Scattering to the Continuum*

Above an excitation energy of 4.29 MeV, the level density in $^{54}$Fe becomes large enough so that with our resolution the extraction of cross sections for inelastic scattering to groups of levels or to bands of excitation energy did not seem fruitful. Instead we treated inelastic scattering to levels of excitation energy greater than 4.29 MeV as inelastic scattering to a structured continuum of levels. Our "continua" are shown in Figure 10 where our angle-averaged double-differentialcross sections for scattering from incident laboratory energy E to outgoing energy dE′ about E′ SIG(E → E′) are plotted versus excitation energy. Clearly levels or groups of levels are preferentially excited at excitation energies of 4.8, 5.4, 5.6 , 6.0, and 6.5 MeV.

The applicability of an evaporation model in describing inelastic scattering to our continua may be judged from Figure 11 whereSIG(E → E′) is plotted versus E′. The straight lines are least squares fits to the data but over a limited range of E′: $E' \leqslant 1.6$ MeV for $E = 8.01$ MeV and $E' \leqslant 2$ MeV for $E = 8.50$ MeV. An evaporation model would seem to offer a fair description of inelastic scattering to levels in the residual nucleus of excitation energy above 6.2 MeV but to be questionable in describing inelastic scattering to levels of lower excitation energy.

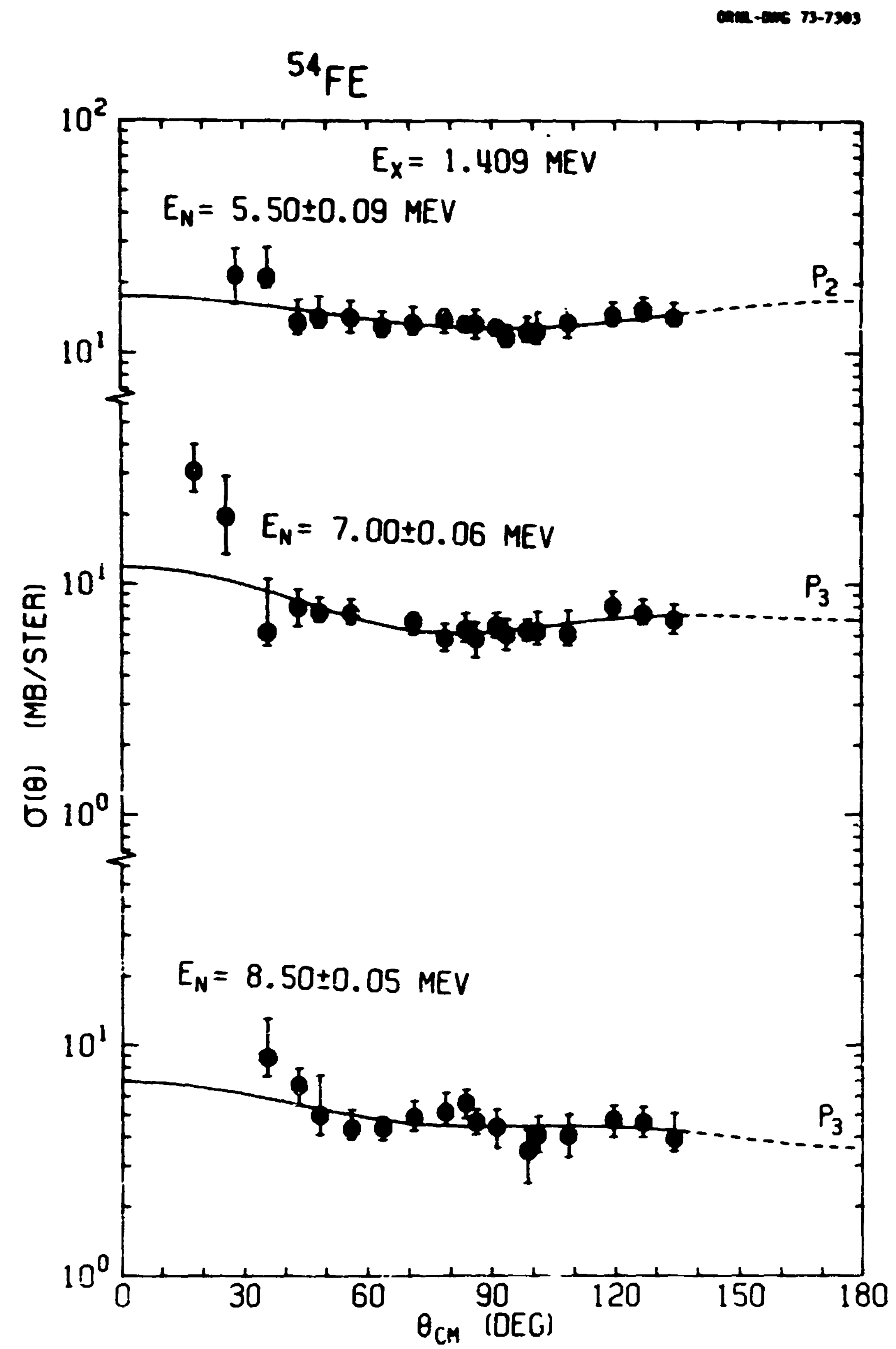


Fig. 4. Our differential center-of-mass cross sections for inelastic scattering to the 1.409 MeV level with Legendre least squares fits to the data.

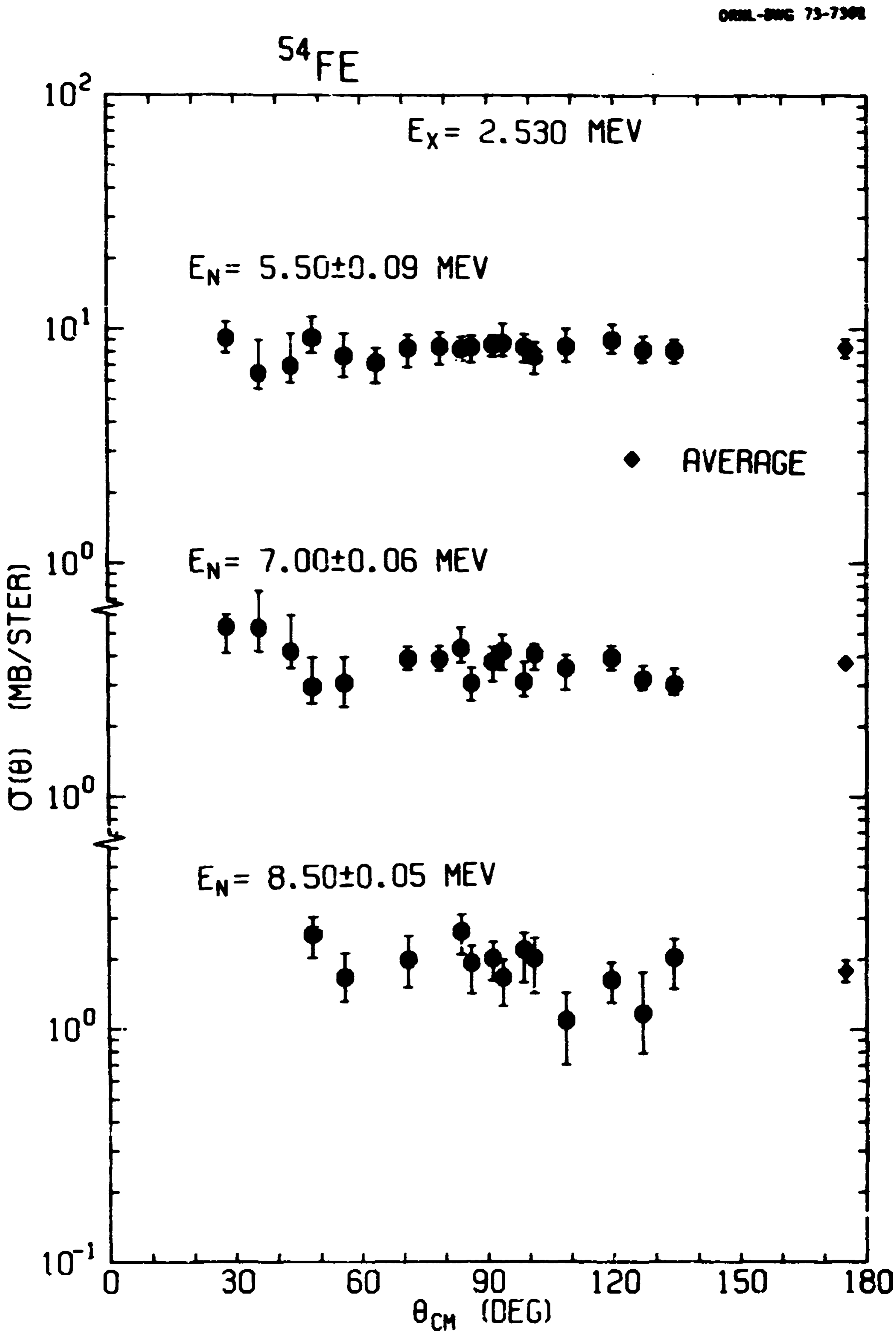


Fig. 5. Our differential center-of-mass cross sections for inelastic scattering to the 2.530 MeV level.

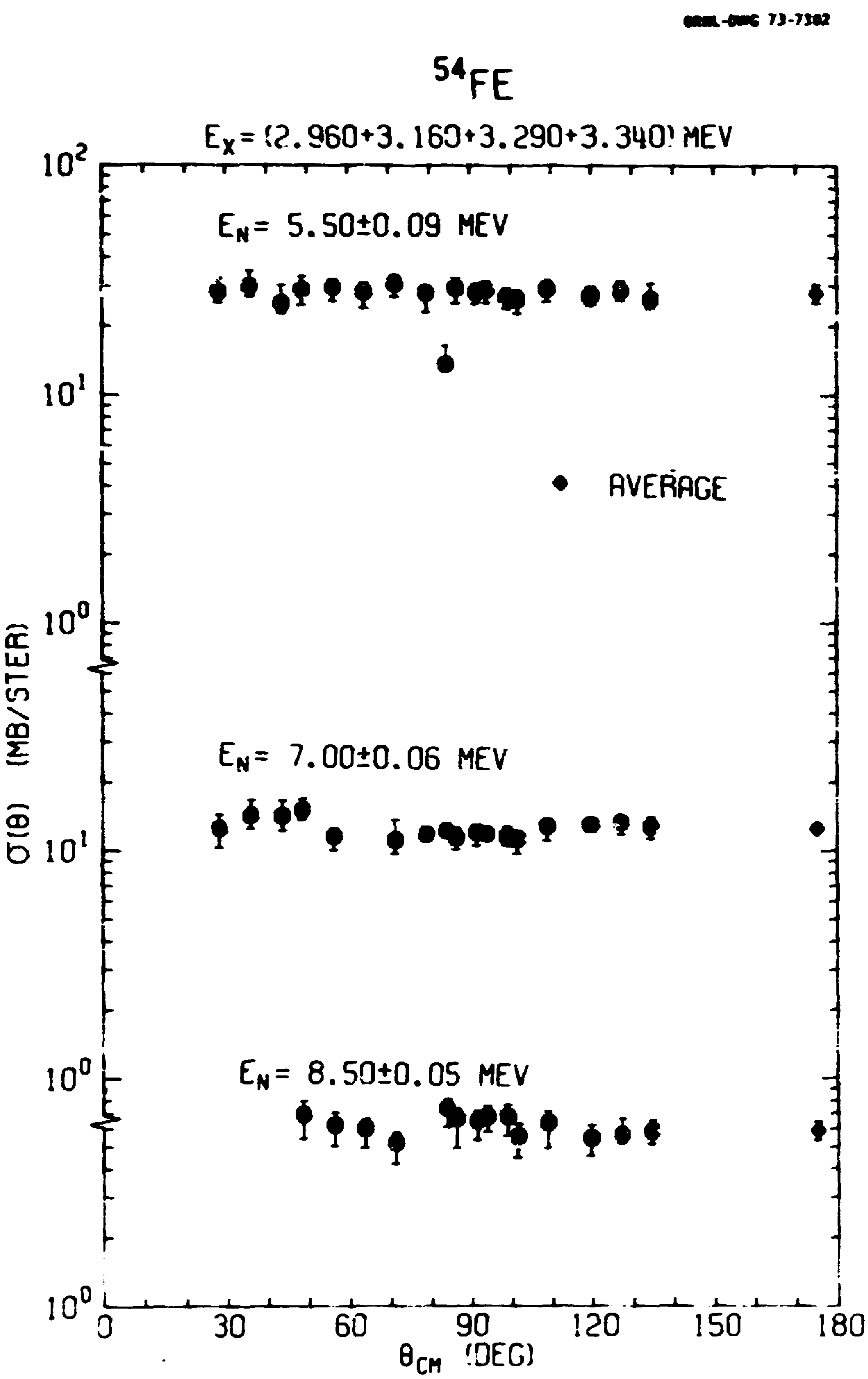


Fig. 6. Our differential center-of-mass cross sections for combined inelastic scattering to the 2.960, 3.160, 3.290, and 3.340 MeV levels.

ORNL-DWG 73-7304

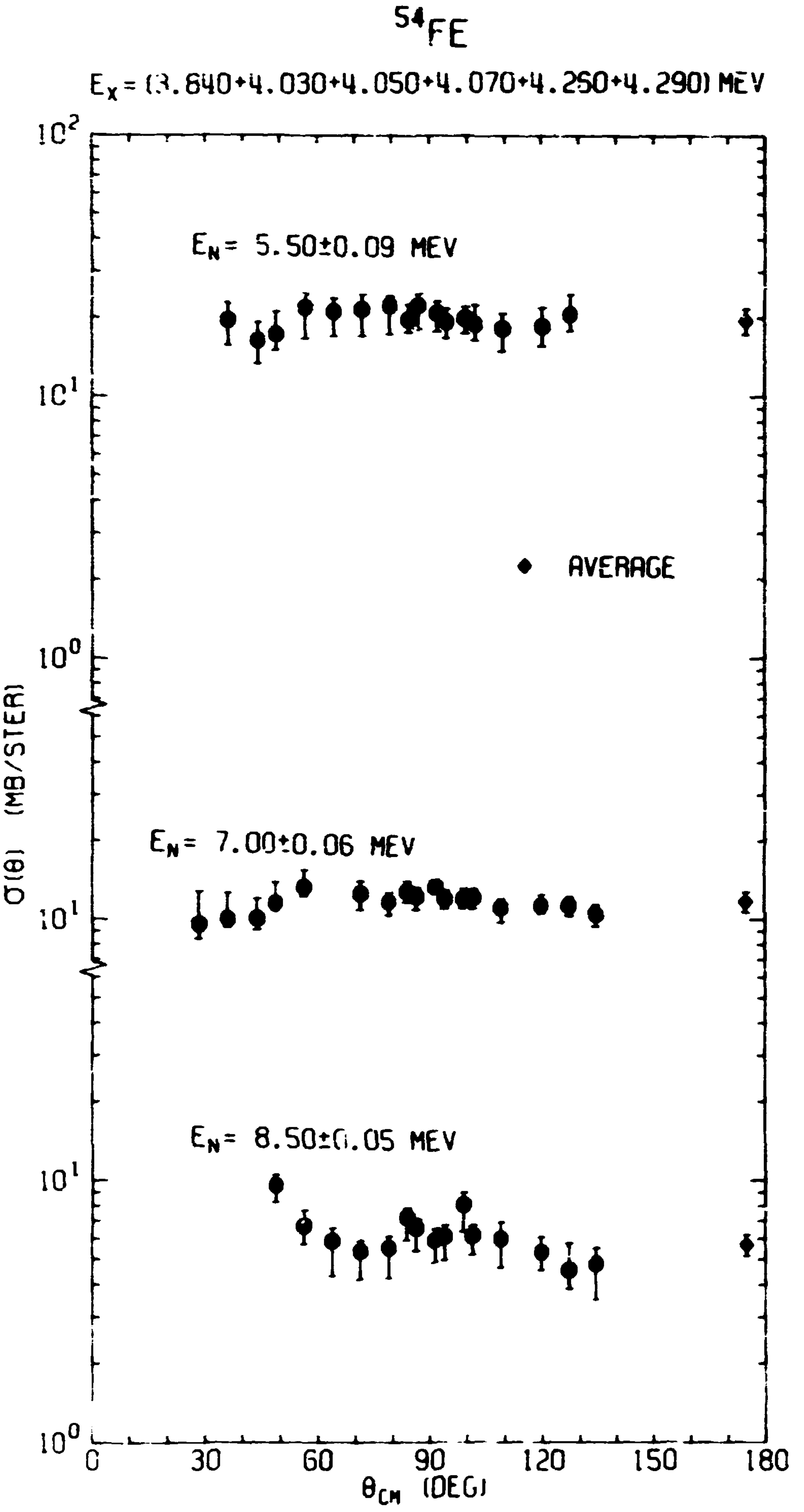


Fig. 7. Our differential center-of-mass cross section for combined inelastic scattering to the 2.960, 3.160, 3.290, and 3.340 MeV levels.

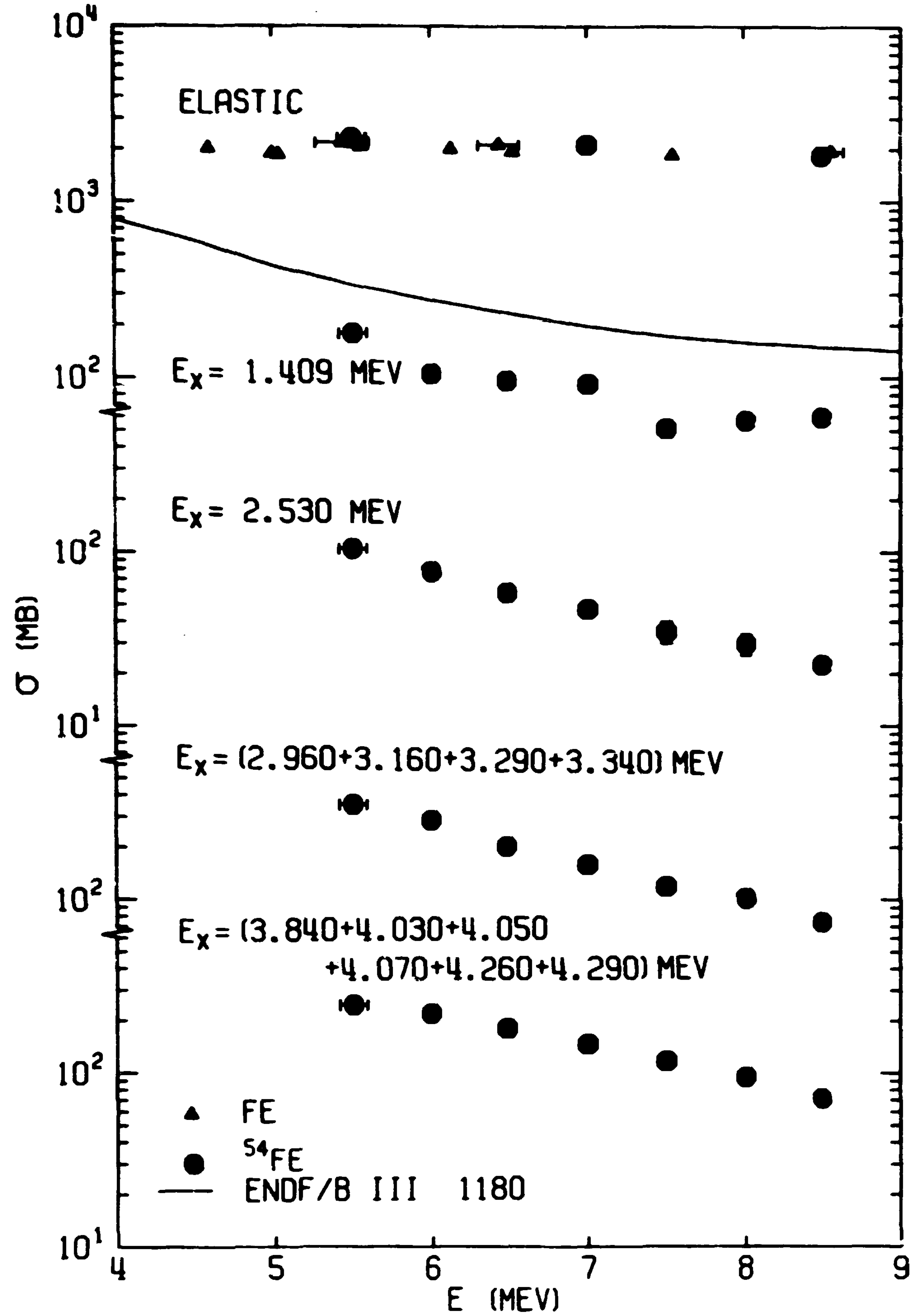


Fig. 8. Our $^{54}$Fe neutron angle-integrated differential cross sections as a function of incident neutron energy. Our previously reported natural iron elastic data are shown. The ENDF/B III MAT 1180 curve for inelastic scattering to the 1.409 MeV level in $^{54}$Fe divided by the $^{54}$Fe natural abundance is given. The ±7% uncertainty in absolute normalization is included in the error bars.

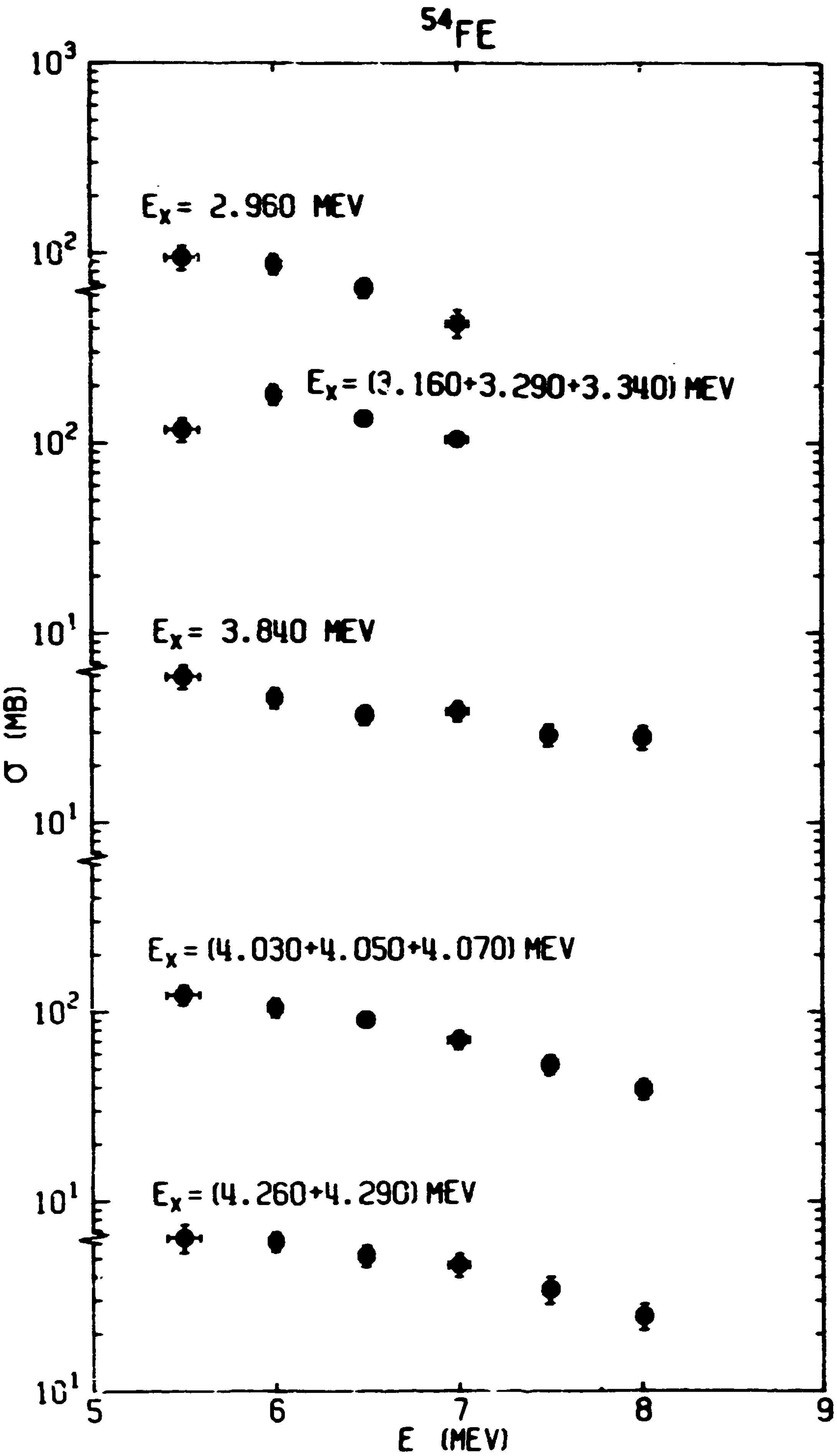


Fig. 9. Our $^{54}Fe$ neutron angle-integrated differential cross sections for inelastic scattering as a function of incident neutron energy. These data are sub-groups of the data given in Figure 8 and do not span the entire range of energy measurements. The ±7% uncertainty in absolute normalization is included in the error bars.

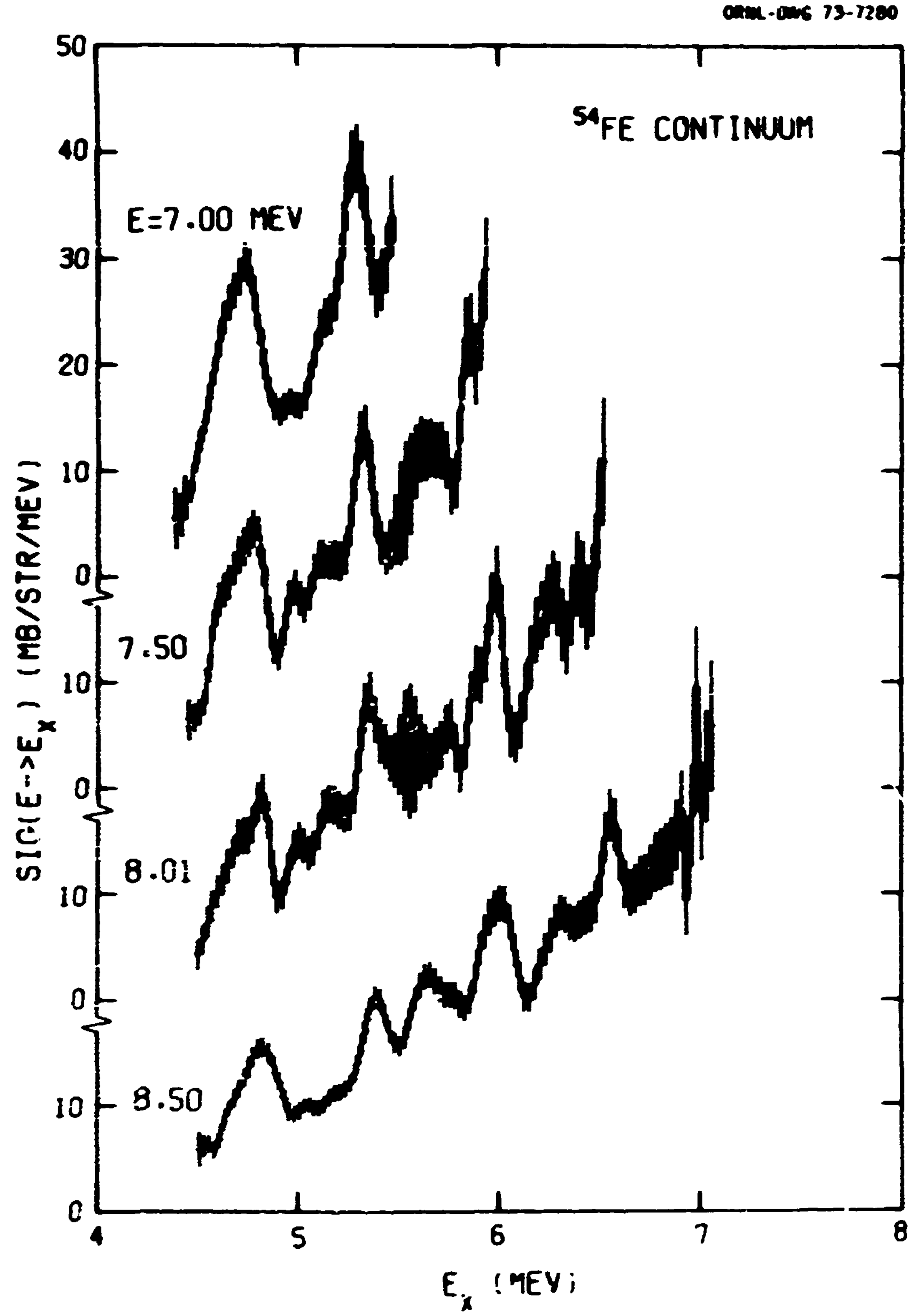


Fig. 10. $^{54}$Fe angle-averaged cross sections for inelastic scattering to the "continuum" as a function of excitation energy for incident neutron energies, E, from 7.00 to 8.50 MeV.

ORNL-DWG 73-7299

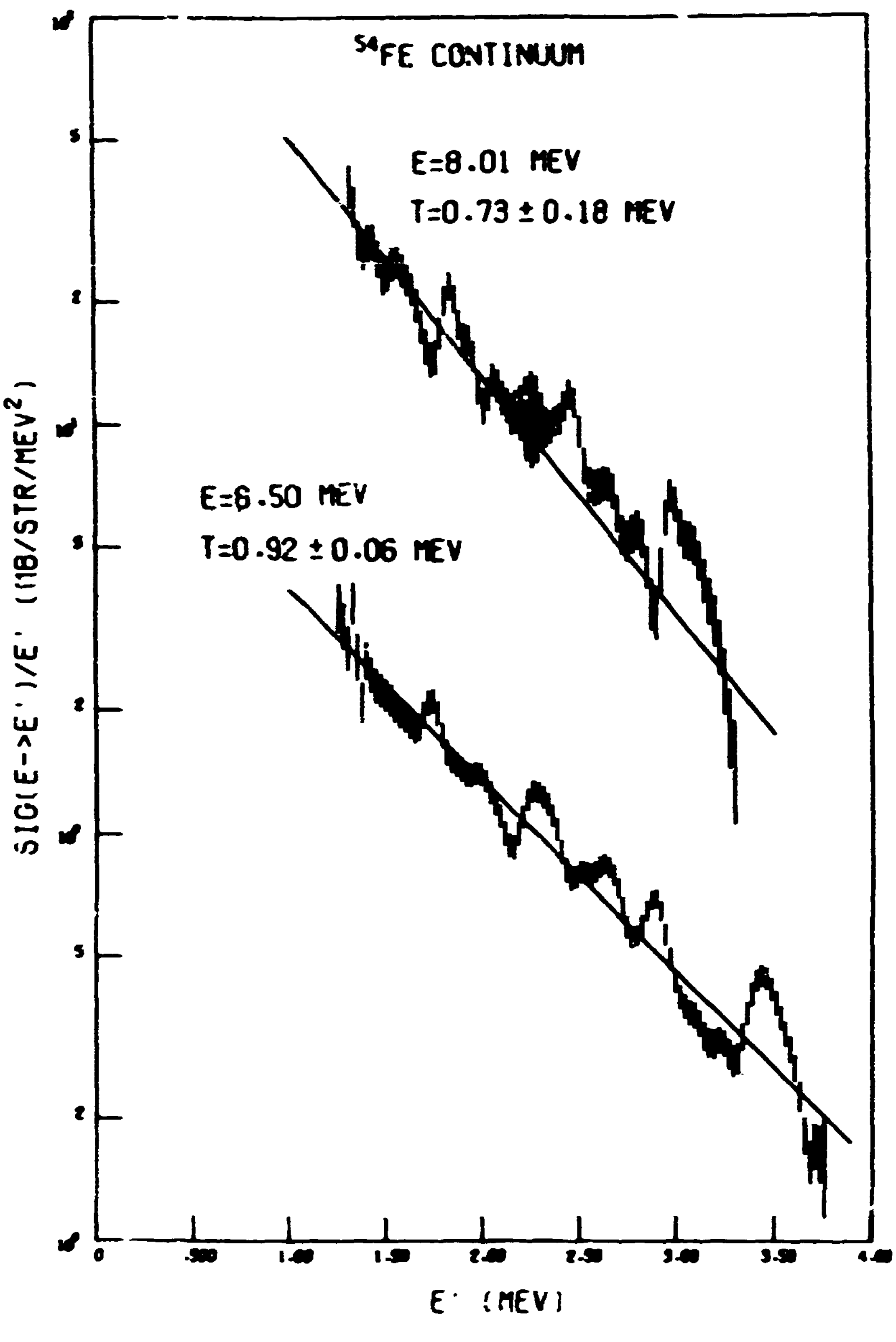


Fig. 11. $^{54}$Fe angle-averaged cross sections for inelastic scattering to the continuum divided by the outgoing neutron energy as a function of outgoing neutron energy. Least squares fits are shown with the resulting temperatures, T. The uncertainties on T are fitting uncertainties only.

## CONCLUSIONS

Our $^{54}$Fe differential elastic scattering cross sections are in good agreement with our previous results for natural iron. The differential cross sections for inelastic scattering to the 1.409 MeV level shows evidence of a direct reaction contribution at the higher incident neutron energies. ENDF/B III MAT 1180 cross sections for inelastic scattering to this level are higher than our data by a factor of 2. An evaporation model for inelastic scattering appears to be adequate for scattering to levels in the residual nucleus of excitation energy greater than 6.2 MeV but is of questionable validity in describing inelastic scattering to levels of lower excitation energy.

## ACKNOWLEDGMENTS

Many have contributed to this experimental program at one time or another and we would like to thank them for their contributions. In particular, we would like to acknowledge the help of J. K. Dickens, J. W. McConnell, J. A. Biggerstaff, A. M. Marusak, P. H. Stelson, C. O. LeRigoleur, and E. Hungerford.

We are deeply indebted to F. C. Maienschein, director of the Neutron Physics Division, for his support of the experiment with the use of computers in report preparation and type setting which produced this report and the other six of our last seven reports.

## REFERENCES

1. F. G. Perey and W. E. Kinney, "Carbon Neutron Elastic- and Inelastic-Scattering Cross Sections from 4.5 to 8. MeV", ORNL-4441 (December 1970).

   F. G. Perey, C. O. LeRigoleur and W. E. Kinney, "Nickel-60 Neutron Elastic- and Inelastic-Scattering Cross Sections from 6.5 to 8.5 MeV". ORNL-4523 (April 1970).

   W. E. Kinney and F. G. Perey, "Neutron Elastic- and Inelastic-Scattering Cross Sections from $^{56}$Fe in the Energy Range 4.19 to 8.56 MeV", ORNL-4515 (June 1970).

   F. G. Perey and W. E. Kinney, "Calcium Neutron Elastic- and Inelastic-Scattering Cross Sections from 4.0 to 8.5 MeV", ORNL-4519 (April 1970).

   F. G. Perey and W. E. Kinney, "Sulfur Neutron Elastic- and Inelastic-Scattering Cross Sections from 4 to 8.5 MeV", ORNL-4539 (June 1970).

   W. E. Kinney and F. G. Perey, "Neutron Elastic- and Inelastic- Scattering Cross Sections for Co in the Energy Range 4.19 to 8.56 MeV", ORNL-4549 (June 1970).

   W. E. Kinney and F. G. Perey, "Neutron Elastic- and Inelastic- Scattering Cross Sections for Mg in the Energy Range 4.19 to 8.56 MeV", ORNL-4550 (June 1970).

   W. E. Kinney and F. G. Perey, "Neutron Elastic- and Inelastic- Scattering Cross Sections for Si in the Energy Range 4.19 to 8.56 MeV", ORNL-4517 (July 1970).

   F. G. Perey and W. E. Kinney, "Neutron Elastic and Inelastic- Scattering Cross Sections for Na in the Energy Range of 5.4 to 8.5 MeV", ORNL-4518 (August 1970).

   W. E. Kinney and F. G. Perey, "Al Neutron Elastic- and Inelastic- Scattering Cross Sections from 4.19 to 8.56 MeV", ORNL-4516 (October 1970).

   F. G. Perey and W. E. Kinney, "V Neutron Elastic- and Inelastic- Scattering Cross Sections from 4.19 to 8.56 MeV", ORNL-4551 (October 1970).

   F. G. Perey and W. E. Kinney, "Neutron Elastic- and Inelastic- Scattering Cross Sections for Yttrium in the Energy Range 4.19 to 8.56 MeV", ORNL-4552 (December 1970).

   W. E. Kinney and F. G. Perey, "Neutron Elastic- and Inelastic- Scattering Cross Sections for Oxygen in the Energy Range 4.34 to 8.56 MeV", ORNL-4780 (April 1972).

   W. E. Kinney and F. G. Perey. "W Neutron Elastic- and Inelastic- Scattering Cross Sections from 4.34 to 8.56 MeV", ORNL-4803 (May 1973).

   W. E. Kinney and F. G. Perey, "$^{238}$U Neutron Elastic-Scattering Cross Sections from 6.44 to 8.56 MeV", ORNL-4804 (June 1973).

   W. E. Kinney and F. G. Perey, "Natural Titanium Neutron Elastic and Inelastic Scattering Cross Sections from 4.07 to 8.56 MeV", ORNL-4810 (October 1973).

W. E. Kinney and F. G. Perey, "Natural Nickel and $^{60}$Ni Neutron Elastic and Inelastic Scattering Cross Sections from 4.07 to 8.56 MeV", ORNL-4807 (November 1973).

W. E. Kinney and F. G. Perey, "Natural Chromium and $^{52}$Cr Neutron Elastic and Inelastic Scattering Cross Sections from 4.07 to 8.56 MeV", ORNL-4806 (November 1973).

F. G. Perey and W. E. Kinney, "Nitrogen Neutron Elastic and Inelastic Scattering Cross Sections from 4.34 to 8.56 MeV", ORNL-4805 (January 1974).

W. E. Kinney and F. G. Perey "$^{63}$Cu and $^{65}$Cu Neutron Elastic and Inelastic Scattering Cross Sections from 5.50 to 8.50 MeV", ORNL-4908 (January 1974).

W. E. Kinney and F. G Perey, "$^{206}$Pb, $^{207}$Pb, and $^{208}$Pb Neutron Elastic and Inelastic Scattering Cross Sections from 5.50 to 8.50 MeV", ORNL-4909 (To be published).

2. W. E. Kinney, "Neutron Elastic and Inelastic Scattering from $^{56}$Fe from 4.60 to 7.55 MeV", ORNL-TM-2052, January 1968.
3. R. E. Textor and V. V. Verbinski, "05S: A Monte Carlo Code for Calculating Pulse Height Distributions Due to Monoenergetic Neutrons Incident on Organic Scintillators", ORNL-4160 (February 1968).
4. W. E. Kinney, Nucl. Instr. and Methods *83*, 15 (1970).
5. S. Cierjacks, P. Forti, D. Kopsch, L. Kropp, J. Nebe, and H. Unseld, "High Resolution Total Neutron Cross Sections Between 0.5 - 30 MeV", EANDC(E) - 111 "U" (June, 1968)

# APPENDIX

## Tabulated Values of $^{54}$Fe Neutron Elastic Scattering Cross Sections and Cross Sections for Inelastic Scattering to Discrete Levels

Our measured values for $^{54}$Fe neutron elastic scattering cross sections and cross sections for inelastic scattering to discrete levels are tabulated below. The uncertainties in differential cross sections, indicated by $\Delta$ in the tables, are relative and do *not* include a $\pm 7\%$ uncertainty in detector efficiency which is common to all points. The $\pm 7\%$ uncertainty is included in the integrated and average values. The total cross sections, gsbT, are those we used in the computation of Wick's Limit and were not measured by us.

We have not included the cross sections for inelastic scattering to the continuum. They are available from the National Neutron Cross Section Center, Brookhaven National Laboratory, or from us.

Average and integrated values for cross sections for inelastic scattering to the 1.409 MeV level measured at only three angles are not given because of the anisotropic angular distributions of neutrons so scattered.

$E_n = 5.50 \pm 0.09$ MeV
Elastic Scattering

| $\theta_{cm}$ deg. | $d\sigma/d\omega$ mb/str | Δ (%) + | Δ (%) − |
|---|---|---|---|
| 13.10 | 2141.25 | 5.1 | 4.5 |
| 20.70 | 1655.05 | 5.3 | 4.9 |
| 28.00 | 1065.67 | 5.7 | 5.1 |
| 28.30 | 1096.10 | 4.8 | 6.0 |
| 35.62 | 662.67 | 4.9 | 5.1 |
| 43.22 | 326.84 | 5.6 | 6.2 |
| 48.29 | 195.01 | 6.4 | 7.0 |
| 55.88 | 70.65 | 9.1 | 10.2 |
| 63.45 | 22.27 | 15.8 | 24.4 |
| 71.00 | 10.59 | 26.4 | 32.0 |
| 78.54 | 15.70 | 25.9 | 20.1 |
| 83.56 | 21.42 | 9.9 | 16.4 |
| 86.07 | 24.52 | 12.5 | 16.3 |
| 91.07 | 29.69 | 10.0 | 11.6 |
| 93.57 | 30.81 | 9.0 | 11.1 |
| 98.56 | 33.94 | 11.6 | 8.7 |
| 101.05 | 36.00 | 7.4 | 9.7 |
| 108.52 | 33.33 | 11.5 | 9.1 |
| 119.44 | 30.66 | 10.9 | 13.4 |
| 126.86 | 24.75 | 12.8 | 12.1 |
| 134.28 | 17.66 | 18.7 | 12.2 |

$\int(d\sigma/d\omega)d\omega$ = 2304.48 mb ± 7.2 %
Wick's Limit = 2218.23 mb ± 9.2 %
$\sigma_T$ = 3.70 b ± 3.0 %

Legendre Fit, Order = 8

| $k$ | $a_k$ | Δ(%) |
|---|---|---|
| 0 | 366.76953 | 1.9 |
| 1 | 286.22949 | 2.2 |
| 2 | 218.97568 | 2.4 |
| 3 | 155.34956 | 2.8 |
| 4 | 87.67975 | 3.9 |
| 5 | 39.48889 | 7.0 |
| 6 | 15.81805 | 12.7 |
| 7 | 4.60644 | 28.3 |
| 8 | 1.22247 | 67.7 |

$E_n = 5.50 \pm 0.09$ MeV
(n,n′) to: 1.409 MeV Level

| $\theta_{cm}$ deg. | $d\sigma/d\omega$ mb/str | Δ (%) + | Δ (%) − |
|---|---|---|---|
| 28.08 | 21.54 | 30.7 | 24.5 |
| 35.72 | 21.16 | 35.1 | 9.5 |
| 43.34 | 13.46 | 25.6 | 10.8 |
| 48.42 | 14.16 | 23.2 | 8.7 |
| 56.02 | 14.19 | 17.9 | 13.5 |
| 63.60 | 12.95 | 16.0 | 8.9 |
| 71.17 | 13.42 | 18.0 | 9.9 |
| 78.71 | 13.90 | 9.9 | 12.7 |
| 83.73 | 13.20 | 7.3 | 10.0 |
| 86.24 | 13.25 | 15.3 | 13.1 |
| 91.24 | 12.80 | 10.8 | 7.5 |
| 93.74 | 11.57 | 13.0 | 7.9 |
| 98.73 | 12.25 | 16.3 | 8.5 |
| 101.22 | 12.26 | 21.9 | 10.7 |
| 108.69 | 13.46 | 16.2 | 13.6 |
| 119.59 | 14.50 | 14.2 | 9.2 |
| 127.01 | 15.29 | 13.7 | 9.3 |
| 134.40 | 14.17 | 16.3 | 6.7 |

$\int(d\sigma/d\omega)d\omega$ = 178.30 mb ± 8.0 %

Legendre Fit, Order = 2

| $k$ | $a_k$ | Δ(%) |
|---|---|---|
| 0 | 28.37712 | 4.0 |
| 1 | 0.17325 | 406.0 |
| 2 | 1.20662 | 46.3 |

$E_n = 5.50 \pm 0.09$ MeV
(n,n′) to: 2.530 MeV Level

| $\theta_{cm}$ | $d\sigma/d\omega$ | Δ (%) | |
|---|---|---|---|
| *deg.* | *mb/str* | + | − |
| 28.18 | 9.12 | 17.2 | 13.3 |
| 35.85 | 6.46 | 38.8 | 14.1 |
| 43.49 | 6.95 | 37.0 | 15.1 |
| 48.58 | 9.15 | 22.9 | 13.8 |
| 56.20 | 7.66 | 24.7 | 18.6 |
| 63.80 | 7.16 | 15.2 | 18.2 |
| 71.38 | 8.25 | 13.9 | 16.8 |
| 78.93 | 8.40 | 14.9 | 15.9 |
| 83.96 | 8.21 | 12.5 | 10.7 |
| 86.45 | 8.36 | 11.8 | 13.8 |
| 91.47 | 8.54 | 9.5 | 10.8 |
| 93.96 | 8.67 | 21.5 | 11.8 |
| 98.96 | 8.36 | 13.6 | 13.7 |
| 101.45 | 7.66 | 14.5 | 15.9 |
| 108.90 | 8.42 | 18.9 | 13.8 |
| 119.79 | 8.97 | 16.7 | 12.1 |
| 127.19 | 8.11 | 14.7 | 10.7 |
| 134.57 | 8.10 | 11.2 | 11.4 |

Avg. $d\sigma/d\omega$ = 8.30 mb/str ± 9.2 %
$\int(d\sigma/d\omega)d\omega$ = 104.34 mb ± 9.2 %

---

$E_n = 5.50 \pm 0.09$ MeV
(n,n′) to: 2.960 MeV Level

| $\theta_{cm}$ | $d\sigma/d\omega$ | Δ (%) | |
|---|---|---|---|
| *deg.* | *mb/str* | + | − |
| 84.07 | 7.62 | 13.7 | 22.6 |
| 91.59 | 7.59 | 11.3 | 17.8 |
| 99.07 | 7.40 | 20.9 | 12.1 |

Avg. $d\sigma/d\omega$ = 7.54 mb/str ± 14.2 %
$\int(d\sigma/d\omega)d\omega$ = 94.74 mb ± 14.2 %

$E_n = 5.50 \pm 0.09$ MeV
(n,n′) to: 2.960 MeV Level
+ 3.160 MeV Level
+ 3.290 MeV Level
+ 3.340 MeV Level

| $\theta_{cm}$ | $d\sigma/d\omega$ | Δ (%) | |
|---|---|---|---|
| *deg.* | *mb/str* | + | − |
| 28.27 | 28.35 | 14.2 | 10.6 |
| 35.95 | 29.71 | 16.8 | 9.8 |
| 43.62 | 25.11 | 20.1 | 9.6 |
| 48.73 | 28.89 | 14.0 | 14.7 |
| 56.37 | 29.67 | 7.7 | 13.1 |
| 63.97 | 28.17 | 9.6 | 15.3 |
| 71.56 | 30.63 | 9.2 | 12.4 |
| 79.13 | 27.90 | 8.0 | 17.8 |
| 84.17 | 13.62 | 20.7 | 6.6 |
| 86.65 | 29.26 | 10.3 | 14.4 |
| 91.67 | 28.02 | 9.0 | 10.9 |
| 94.16 | 28.80 | 8.9 | 12.4 |
| 99.15 | 26.78 | 8.7 | 11.0 |
| 101.64 | 26.13 | 9.3 | 13.3 |
| 109.08 | 29.09 | 8.8 | 12.3 |
| 119.96 | 27.08 | 9.7 | 8.9 |
| 127.34 | 28.60 | 10.3 | 9.5 |
| 134.70 | 26.17 | 17.2 | 8.7 |

Avg. $d\sigma/d\omega$ = 27.90 mb/str ± 9.5 %
$\int(d\sigma/d\omega)d\omega$ = 350.63 mb ± 9.5 %

Data at the Following Angles
Excluded from the Average:
84.17

---

$E_n = 5.50 \pm 0.09$ MeV
(n,n′) to: 3.160 MeV Level

| $\theta_{cm}$ | $d\sigma/d\omega$ | Δ (%) | |
|---|---|---|---|
| *deg.* | *mb/str* | + | − |
| 91.66 | 8.56 | 14.9 | 25.6 |
| 99.14 | 7.13 | 7.3 | 22.7 |

Avg. $d\sigma/d\omega$ = 7.16 mb/str ± 10.1 %
$\int(d\sigma/d\omega)d\omega$ = 89.99 mb ± 10.1 %

$E_n = 5.50 \pm 0.09$ MeV
(n,n′) to: 4.260 MeV Level
+ 4.290 MeV Level

| $\theta_{cm}$ | $d\sigma/d\omega$ | $\Delta$ (%) | |
|---|---|---|---|
| *deg.* | *mb/str* | + | − |
| 84.81 | 4.55 | 21.8 | 27.2 |
| 92.33 | 6.02 | 13.7 | 27.6 |
| 99.80 | 5.48 | 13.6 | 21.1 |

Avg. $d\sigma/d\omega$ = 5.12 mb/str ± 16.9 %
$\int(d\sigma/d\omega)d\omega$ = 64.37 mb ± 16.9 %

---

$E_n = 6.00 \pm 0.04$ MeV
(n,n′) to: 1.409 MeV Level

| $\theta_{cm}$ | $d\sigma/d\omega$ | $\Delta$ (%) | |
|---|---|---|---|
| *deg.* | *mb/str* | + | − |
| 83.71 | 7.69 | 8.8 | 8.4 |
| 91.22 | 9.08 | 10.8 | 8.8 |
| 98.71 | 9.08 | 17.8 | 11.5 |

---

$E_n = 6.00 \pm 0.04$ MeV
(n,n′) to: 2.530 MeV Level

| $\theta_{cm}$ | $d\sigma/d\omega$ | $\Delta$ (%) | |
|---|---|---|---|
| *deg.* | *mb/str* | + | − |
| 83.90 | 5.53 | 18.8 | 13.8 |
| 91.41 | 6.50 | 9.4 | 13.1 |
| 98.90 | 6.13 | 16.2 | 9.7 |

Avg. $d\sigma/d\omega$ = 6.13 mb/str ± 10.6 %
$\int(d\sigma/d\omega)d\omega$ = 77.01 mb ± 10.6 %

---

$E_n = 6.00 \pm 0.04$ MeV
(n,n′) to: 2.960 MeV Level

| $\theta_{cm}$ | $d\sigma/d\omega$ | $\Delta$ (%) | |
|---|---|---|---|
| *deg.* | *mb/str* | + | − |
| 83.99 | 6.67 | 12.2 | 15.2 |
| 91.51 | 7.21 | 9.4 | 18.3 |
| 98.99 | 7.26 | 13.3 | 13.2 |

Avg. $d\sigma/d\omega$ = 6.96 mb/str ± 11.4 %
$\int(d\sigma/d\omega)d\omega$ = 87.52 mb ± 11.4 %

$E_n = 6.00 \pm 0.04$ MeV
(n,n′) to: 2.960 MeV Level
+ 3.160 MeV Level
+ 3.290 MeV Level
+ 3.340 MeV Level

| $\theta_{cm}$ | $d\sigma/d\omega$ | $\Delta$ (%) | |
|---|---|---|---|
| *deg.* | *mb/str* | + | − |
| 84.05 | 22.37 | 10.8 | 9.1 |
| 91.57 | 23.22 | 10.4 | 9.6 |
| 99.05 | 22.44 | 6.7 | 10.5 |

Avg. $d\sigma/d\omega$ = 22.57 mb/str ± 9.4 %
$\int(d\sigma/d\omega)d\omega$ = 283.67 mb ± 9.4 %

---

$E_n = 6.00 \pm 0.04$ MeV
(n,n′) to: 3.160 MeV Level
+ 3.290 MeV Level
+ 3.340 MeV Level

| $\theta_{cm}$ | $d\sigma/d\omega$ | $\Delta$ (%) | |
|---|---|---|---|
| *deg.* | *mb/str* | + | − |
| 84.08 | 14.72 | 7.8 | 15.9 |
| 91.59 | 15.14 | 9.7 | 18.8 |
| 99.08 | 14.06 | 10.5 | 13.3 |

Avg. $d\sigma/d\omega$ = 14.36 mb/str ± 11.2 %
$\int(d\sigma/d\omega)d\omega$ = 180.45 mb ± 11.2 %

---

$E_n = 6.00 \pm 0.04$ MeV
(n,n′) to: 3.840 MeV Level

| $\theta_{cm}$ | $d\sigma/d\omega$ | $\Delta$ (%) | |
|---|---|---|---|
| *deg.* | *mb/str* | + | − |
| 84.28 | 3.54 | 14.2 | 13.8 |
| 91.80 | 3.60 | 14.4 | 16.7 |
| 99.28 | 3.76 | 20.1 | 14.4 |

Avg. $d\sigma/d\omega$ = 3.63 mb/str ± 12.0 %
$\int(d\sigma/d\omega)d\omega$ = 45.58 mb ± 12.0 %

$E_n = 5.50 \pm 0.09$ MeV
(n,n′) to: 3.160 MeV Level
+ 3.290 MeV Level
+ 3.340 MeV Level

| $\theta_{cm}$ | $d\sigma/d\omega$ | $\Delta$ (%) | |
|---|---|---|---|
| *deg.* | *mb/str* | + | − |
| 84.19 | 9.38 | 12.0 | 12.0 |

Avg. $d\sigma/d\omega$ = 9.38 mb/str ± 13.9 %
$\int(d\sigma/d\omega)d\omega$ = 117.87 mb ± 13.9 %

---

$E_n = 5.50 \pm 0.09$ MeV
(n,n′) to: 3.290 MeV Level
+ 3.340 MeV Level

| $\theta_{cm}$ | $d\sigma/d\omega$ | $\Delta$ (%) | |
|---|---|---|---|
| *deg.* | *mb/str* | + | − |
| 91.73 | 11.69 | 7.1 | 19.8 |
| 99.21 | 11.08 | 10.3 | 22.7 |

Avg. $d\sigma/d\omega$ = 11.17 mb/str ± 12.0 %
$\int(d\sigma/d\omega)d\omega$ = 140.36 mb ± 12.0 %

---

$E_n = 5.50 \pm 0.09$ MeV
(n,n′) to: 3.840 MeV Level

| $\theta_{cm}$ | $d\sigma/d\omega$ | $\Delta$ (%) | |
|---|---|---|---|
| *deg.* | *mb/str* | + | − |
| 84.47 | 4.43 | 17.5 | 21.5 |
| 91.99 | 5.37 | 12.7 | 21.0 |
| 99.46 | 4.65 | 23.6 | 11.8 |

Avg. $d\sigma/d\omega$ = 4.71 mb/str ± 14.7 %
$\int(d\sigma/d\omega)d\omega$ = 59.13 mb ± 14.7 %

$E_n = 5.50 \pm 0.09$ MeV
(n,n′) to: 3.840 MeV Level
+ 4.030 MeV Level
+ 4.050 MeV Level
+ 4.070 MeV Level
+ 4.260 MeV Level
+ 4.290 MeV Level

| $\theta_{cm}$ | $d\sigma/d\omega$ | $\Delta$ (%) | |
|---|---|---|---|
| *deg.* | *mb/str* | + | − |
| 36.25 | 19.58 | 16.9 | 19.7 |
| 43.95 | 16.36 | 17.0 | 18.4 |
| 49.10 | 17.28 | 21.6 | 13.1 |
| 56.78 | 21.88 | 13.0 | 23.8 |
| 64.40 | 21.14 | 12.3 | 19.5 |
| 72.01 | 21.56 | 14.0 | 21.0 |
| 79.62 | 22.23 | 8.8 | 22.2 |
| 84.63 | 19.67 | 14.1 | 10.5 |
| 87.13 | 22.31 | 11.0 | 18.8 |
| 92.15 | 20.89 | 10.5 | 15.0 |
| 94.63 | 19.33 | 12.1 | 13.4 |
| 99.62 | 19.91 | 10.5 | 12.4 |
| 102.12 | 18.95 | 18.1 | 13.5 |
| 109.54 | 18.21 | 14.0 | 18.2 |
| 120.39 | 18.60 | 17.8 | 15.9 |
| 127.75 | 20.68 | 18.9 | 13.5 |

Avg. $d\sigma/d\omega$ = 19.54 mb/str ± 11.1 %
$\int(d\sigma/d\omega)d\omega$ = 245.49 mb ± 11.1 %

---

$E_n = 5.50 \pm 0.09$ MeV
(n,n′) to: 4.030 MeV Level
+ 4.050 MeV Level
+ 4.070 MeV Level

| $\theta_{cm}$ | $d\sigma/d\omega$ | $\Delta$ (%) | |
|---|---|---|---|
| *deg.* | *mb/str* | + | − |
| 84.63 | 10.07 | 12.1 | 17.9 |
| 92.15 | 9.93 | 15.2 | 17.3 |
| 99.62 | 9.75 | 10.1 | 14.5 |

Avg. $d\sigma/d\omega$ = 9.81 mb/str ± 11.8 %
$\int(d\sigma/d\omega)d\omega$ = 123.30 mb ± 11.8 %

$E_n = 6.00 \pm 0.04$ MeV
(n,n') to: 3.840 MeV Level
+ 4.030 MeV Level
+ 4.050 MeV Level
+ 4.070 MeV Level
+ 4.260 MeV Level
+ 4.290 MeV Level

| $\theta_{cm}$ | $d\sigma/d\omega$ | $\Delta$ (%) | |
|---|---|---|---|
| *deg.* | *mb/str* | + | − |
| 84.40 | 16.33 | 11.3 | 12.2 |
| 91.92 | 18.81 | 10.0 | 10.6 |
| 99.39 | 17.58 | 10.4 | 9.5 |

Avg. $d\sigma/d\omega$ = 17.54 mb/str ± 10.6%
$\int(d\sigma/d\omega)d\omega$ = 220.37 mb ± 10.6 %

---

$E_n = 6.00 \pm 0.04$ MeV
(n,n') to: 4.030 MeV Level
+ 4.050 MeV Level
+ 4.070 MeV Level

| $\theta_{cm}$ | $d\sigma/d\omega$ | $\Delta$ (%) | |
|---|---|---|---|
| *deg.* | *mb/str* | + | − |
| 84.39 | 8.23 | 9.8 | 15.1 |
| 91.91 | 9.13 | 11.1 | 16.5 |
| 99.38 | 8.46 | 15.9 | 12.8 |

Avg. $d\sigma/d\omega$ = 8.40 mb/str ± 11.1 %
$\int(d\sigma/d\omega)d\omega$ = 105.51 mb ± 11.1 %

---

$E_n = 6.00 \pm 0.04$ MeV
(n,n') to: 4.260 MeV Level
+ 4.290 MeV Level

| $\theta_{cm}$ | $d\sigma/d\omega$ | $\Delta$ (%) | |
|---|---|---|---|
| *deg.* | *mb/str* | + | − |
| 84.51 | 4.83 | 9.6 | 24.7 |
| 92.03 | 5.54 | 21.6 | 23.7 |
| 99.50 | 5.19 | 13.2 | 22.3 |

Avg. $d\sigma/d\omega$ = 4.91 mb/str ± 11.5 %
$\int(d\sigma/d\omega)d\omega$ = 61.68 mb ± 11.5 %

$E_n = 6.49 \pm 0.04$ MeV
(n,n') to: 1.409 MeV Level

| $\theta_{cm}$ | $d\sigma/d\omega$ | $\Delta$ (%) | |
|---|---|---|---|
| *deg.* | *mb/str* | + | − |
| 83.69 | 7.50 | 10.1 | 9.5 |
| 91.21 | 8.12 | 13.2 | 13.4 |
| 98.70 | 7.30 | 15.8 | 9.7 |

---

$E_n = 6.49 \pm 0.04$ MeV
(n,n') to: 2.530 MeV Level

| $\theta_{cm}$ | $d\sigma/d\omega$ | $\Delta$ (%) | |
|---|---|---|---|
| *deg.* | *mb/str* | + | − |
| 83.86 | 4.74 | 12.3 | 11.3 |
| 91.37 | 4.90 | 7.3 | 11.3 |
| 98.85 | 4.25 | 12.7 | 9.5 |

Avg. $d\sigma/d\omega$ = 4.63 mb/str ± 10.4%
$\int(d\sigma/d\omega)d\omega$ = 58.18 mb ± 10.4 %

---

$E_n = 6.49 \pm 0.04$ MeV
(n,n') to: 2.960 MeV Level

| $\theta_{cm}$ | $d\sigma/d\omega$ | $\Delta$ (%) | |
|---|---|---|---|
| *deg.* | *mb/str* | + | − |
| 83.93 | 5.28 | 8.7 | 13.2 |
| 91.45 | 5.27 | 9.6 | 16.3 |
| 98.94 | 5.12 | 12.3 | 20.0 |

Avg. $d\sigma/d\omega$ = 5.21 mb/str ± 11.1%
$\int(d\sigma/d\omega)d\omega$ = 65.45 mb ± 11.1 %

$E_n = 6.49 \pm 0.04$ MeV
(n,n′) to: 2.960 MeV Level
+ 3.160 MeV Level
+ 3.290 MeV Level
+ 3.340 MeV Level

| $\theta_{cm}$ | $d\sigma/d\omega$ | $\Delta$ (%) | |
|---|---|---|---|
| *deg.* | *mb/str* | + | − |
| 83.98 | 15.93 | 12.4 | 8.7 |
| 91.50 | 16.11 | 7.6 | 9.2 |
| 98.98 | 15.90 | 7.2 | 12.0 |

Avg. $d\sigma/d\omega$ = 15.96 mb/str ± 9.3 %
$\int(d\sigma/d\omega)d\omega$ = 200.59 mb ± 9.3 %

---

$E_n = 6.49 \pm 0.04$ MeV
(n,n′) to: 3.160 MeV Level
+ 3.290 MeV Level
+ 3.340 MeV Level

| $\theta_{cm}$ | $d\sigma/d\omega$ | $\Delta$ (%) | |
|---|---|---|---|
| *deg.* | *mb/str* | + | − |
| 84.01 | 10.66 | 7.1 | 17.8 |
| 91.52 | 10.82 | 9.5 | 15.0 |
| 99.00 | 10.88 | 9.3 | 12.4 |

Avg. $d\sigma/d\omega$ = 10.71 mb/str ± 9.5 %
$\int(d\sigma/d\omega)d\omega$ = 134.58 mb ± 9.5 %

---

$E_n = 6.49 \pm 0.04$ MeV
(n,n′) to: 3.840 MeV Level

| $\theta_{cm}$ | $d\sigma/d\omega$ | $\Delta$ (%) | |
|---|---|---|---|
| *deg.* | *mb/str* | + | − |
| 84.17 | 3.03 | 19.7 | 13.7 |
| 91.68 | 2.96 | 17.8 | 12.2 |
| 99.16 | 2.83 | 15.2 | 16.2 |

Avg. $d\sigma/d\omega$ = 2.95 mb/str ± 11.2 %
$\int(d\sigma/d\omega)d\omega$ = 37.03 mb ± 11.2 %

$E_n = 6.49 \pm 0.04$ MeV
(n,n′) to: 3.840 MeV Level
+ 4.030 MeV Level
+ 4.050 MeV Level
+ 4.070 MeV Level
+ 4.260 MeV Level
+ 4.290 MeV Level

| $\theta_{cm}$ | $d\sigma/d\omega$ | $\Delta$ (%) | |
|---|---|---|---|
| *deg.* | *mb/str* | + | − |
| 84.25 | 14.74 | 7.4 | 9.5 |
| 91.76 | 14.22 | 9.5 | 9.6 |
| 99.24 | 14.32 | 8.1 | 8.4 |

Avg. $d\sigma/d\omega$ = 14.40 mb/str ± 9.7 %
$\int(d\sigma/d\omega)d\omega$ = 180.90 mb ± 9.7 %

---

$E_n = 6.49 \pm 0.04$ MeV
(n,n′) to: 4.030 MeV Level
+ 4.050 MeV Level
+ 4.070 MeV Level

| $\theta_{cm}$ | $d\sigma/d\omega$ | $\Delta$ (%) | |
|---|---|---|---|
| *deg.* | *mb/str* | + | − |
| 84.24 | 6.93 | 14.3 | 10.2 |
| 91.76 | 7.13 | 10.6 | 11.1 |
| 99.24 | 7.47 | 8.6 | 9.9 |

Avg. $d\sigma/d\omega$ = 7.23 mb/str ± 10.4 %
$\int(d\sigma/d\omega)d\omega$ = 90.88 mb ± 10.4 %

---

$E_n = 6.49 \pm 0.04$ MeV
(n,n′) to: 4.260 MeV Level
+ 4.290 MeV Level

| $\theta_{cm}$ | $d\sigma/d\omega$ | $\Delta$ (%) | |
|---|---|---|---|
| *deg.* | *mb/str* | + | − |
| 84.33 | 4.17 | 10.3 | 13.3 |
| 91.85 | 4.01 | 17.0 | 25.7 |
| 99.33 | 4.21 | 15.9 | 18.9 |

Avg. $d\sigma/d\omega$ = 4.13 mb/str ± 12.5 %
$\int(d\sigma/d\omega)d\omega$ = 51.90 mb ± 12.5 %

$E_n = 7.00 \pm 0.06$ MeV
Elastic Scattering

| $\theta_{cm}$ deg. | $d\sigma/d\omega$ mb/str | Δ (%) + | − |
|---|---|---|---|
| 13.10 | 2322.48 | 4.2 | 5.2 |
| 20.70 | 1698.86 | 4.8 | 4.5 |
| 27.99 | 1023.24 | 5.2 | 4.6 |
| 28.30 | 1040.05 | 6.8 | 5.0 |
| 35.61 | 562.45 | 5.0 | 5.1 |
| 43.22 | 248.85 | 5.7 | 6.4 |
| 48.29 | 131.32 | 6.7 | 6.6 |
| 55.87 | 35.68 | 11.4 | 12.1 |
| 71.00 | 6.80 | 31.5 | 35.1 |
| 78.54 | 11.31 | 19.7 | 17.4 |
| 83.56 | 15.69 | 10.2 | 13.6 |
| 86.06 | 16.22 | 11.5 | 11.9 |
| 91.07 | 18.88 | 10.2 | 9.6 |
| 93.57 | 19.00 | 12.8 | 10.5 |
| 98.56 | 19.15 | 9.7 | 10.3 |
| 101.05 | 20.41 | 10.4 | 10.5 |
| 108.52 | 17.83 | 12.6 | 11.4 |
| 119.44 | 11.97 | 13.3 | 15.9 |
| 126.86 | 9.70 | 16.0 | 16.9 |
| 134.27 | 5.39 | 33.2 | 28.0 |

$\int(d\sigma/d\omega)d\omega$ = 2107.41 mb ± 7.3 %
Wick's Limit = 2555.19 mb ± 9.2 %
$\sigma_T$ = 3.52 b ± 3.0 %

Legendre Fit, Order = 8

| $k$ | $a_k$ | Δ(%) |
|---|---|---|
| 0 | 335.40552 | 2.0 |
| 1 | 281.74829 | 2.1 |
| 2 | 222.69064 | 2.3 |
| 3 | 162.53687 | 2.6 |
| 4 | 101.53685 | 3.2 |
| 5 | 52.37892 | 4.8 |
| 6 | 23.33212 | 7.7 |
| 7 | 8.15927 | 13.4 |
| 8 | 2.04963 | 28.6 |

$E_n = 7.00 \pm 0.06$ MeV
(n,n') to: 1.409 MeV Level

| $\theta_{cm}$ deg. | $d\sigma/d\omega$ mb/str | Δ (%) + | − |
|---|---|---|---|
| 17.87 | 30.73 | 30.9 | 18.4 |
| 25.51 | 19.55 | 50.1 | 31.2 |
| 35.69 | 6.16 | 71.1 | 12.5 |
| 43.31 | 7.90 | 19.7 | 17.0 |
| 48.38 | 7.51 | 16.0 | 8.2 |
| 55.98 | 7.43 | 15.2 | 9.6 |
| 71.12 | 6.87 | 8.8 | 12.0 |
| 78.67 | 5.77 | 15.9 | 11.8 |
| 83.68 | 6.31 | 17.8 | 11.3 |
| 86.19 | 5.75 | 17.5 | 16.9 |
| 91.19 | 6.54 | 14.2 | 10.2 |
| 93.70 | 5.97 | 17.0 | 13.7 |
| 98.68 | 6.25 | 11.7 | 9.2 |
| 101.18 | 6.18 | 21.7 | 12.1 |
| 108.64 | 6.03 | 26.6 | 10.7 |
| 119.55 | 7.98 | 16.1 | 10.3 |
| 126.97 | 7.40 | 15.5 | 9.3 |
| 134.37 | 6.99 | 16.8 | 12.9 |

$\int(d\sigma/d\omega)d\omega$ = 91.00 mb ± 8.2 %

Legendre Fit, Order = 3

| $k$ | $a_k$ | Δ(%) |
|---|---|---|
| 0 | 14.48305 | 4.2 |
| 1 | 0.67472 | 78.6 |
| 2 | 0.86717 | 36.3 |
| 3 | 0.39655 | 80.3 |

$E_n = 7.00 \pm 0.06$ MeV
(n,n′) to: 2.530 MeV Level

| $\theta_{cm}$ deg. | $d\sigma/d\omega$ mb/str | Δ (%) + | − |
|---|---|---|---|
| 28.12 | 5.32 | 12.9 | 22.9 |
| 35.77 | 5.27 | 44.4 | 20.7 |
| 43.41 | 4.17 | 43.3 | 14.9 |
| 48.49 | 2.95 | 33.6 | 15.3 |
| 56.10 | 3.07 | 29.0 | 21.0 |
| 71.26 | 3.90 | 12.6 | 10.3 |
| 78.81 | 3.89 | 13.6 | 10.8 |
| 83.83 | 4.33 | 22.7 | 13.3 |
| 86.34 | 3.07 | 16.5 | 15.8 |
| 91.34 | 3.79 | 15.6 | 17.7 |
| 93.85 | 4.21 | 17.5 | 16.7 |
| 98.82 | 3.12 | 21.6 | 13.4 |
| 101.33 | 4.10 | 10.1 | 14.4 |
| 108.78 | 3.57 | 13.5 | 19.4 |
| 119.69 | 3.96 | 12.2 | 11.5 |
| 127.09 | 3.20 | 14.5 | 9.5 |
| 134.48 | 3.05 | 17.1 | 9.7 |

Avg. $d\sigma/d\omega$ = 3.73 mb/str ± 9.0 %
$\int(d\sigma/d\omega)d\omega$ = 46.84 mb ± 9.0 %

---

$E_n = 7.00 \pm 0.06$ MeV
(n,n′) to: 2.960 MeV Level

| $\theta_{cm}$ deg. | $d\sigma/d\omega$ mb/str | Δ (%) + | − |
|---|---|---|---|
| 91.40 | 3.68 | 10.9 | 22.6 |
| 98.89 | 3.24 | 18.9 | 18.9 |

Avg. $d\sigma/d\omega$ = 3.40 mb/str ± 16.4 %
$\int(d\sigma/d\omega)d\omega$ = 42.69 mb ± 16.4 %

$E_n = 7.00 \pm 0.06$ MeV
(n,n′) to: 2.960 MeV Level
+ 3.160 MeV Level
+ 3.290 MeV Level
+ 3.340 MeV Level

| $\theta_{cm}$ deg. | $d\sigma/d\omega$ mb/str | Δ (%) + | − |
|---|---|---|---|
| 28.17 | 12.57 | 14.6 | 18.0 |
| 35.83 | 14.26 | 16.7 | 12.4 |
| 43.48 | 14.22 | 16.7 | 13.8 |
| 48.57 | 15.14 | 11.8 | 9.3 |
| 56.19 | 11.55 | 8.5 | 13.0 |
| 71.36 | 11.11 | 22.7 | 12.9 |
| 78.92 | 11.84 | 9.3 | 8.8 |
| 83.93 | 12.27 | 8.1 | 8.7 |
| 86.44 | 11.39 | 10.0 | 11.1 |
| 91.45 | 12.05 | 7.7 | 12.7 |
| 93.96 | 11.82 | 8.7 | 7.1 |
| 98.93 | 11.59 | 10.1 | 8.9 |
| 101.43 | 11.25 | 8.3 | 13.8 |
| 108.89 | 12.81 | 7.4 | 13.5 |
| 119.78 | 13.00 | 10.7 | 5.0 |
| 127.18 | 13.33 | 7.2 | 11.5 |
| 134.56 | 12.72 | 10.2 | 11.2 |

Avg. $d\sigma/d\omega$ = 12.53 mb/str ± 8.5 %
$\int(d\sigma/d\omega)d\omega$ = 157.49 mb ± 8.5 %

---

$E_n = 7.00 \pm 0.06$ MeV
(n,n′) to: 3.160 MeV Level
+ 3.290 MeV Level
+ 3.340 MeV Level

| $\theta_{cm}$ deg. | $d\sigma/d\omega$ mb/str | Δ (%) + | − |
|---|---|---|---|
| 91.47 | 8.13 | 11.4 | 13.2 |
| 98.95 | 8.47 | 11.3 | 8.9 |

Avg. $d\sigma/d\omega$ = 8.34 mb/str ± 10.4 %
$\int(d\sigma/d\omega)d\omega$ = 104.84 mb ± 10.4 %

$E_n = 7.00 \pm 0.06$ MeV
(n,n') to: 3.840 MeV Level

| $\theta_{cm}$ deg. | $d\sigma/d\omega$ mb/str | $\Delta$ (%) + | $\Delta$ (%) − |
|---|---|---|---|
| 84.08 | 3.37 | 11.7 | 15.7 |
| 91.59 | 2.97 | 12.5 | 10.4 |
| 99.08 | 3.03 | 19.3 | 14.1 |

Avg. $d\sigma/d\omega$ = 3.08 mb/str ± 11.8 %
$\int(d\sigma/d\omega)d\omega$ = 38.75 mb ± 11.8 %

---

$E_n = 7.00 \pm 0.06$ MeV
(n,n') to: 3.840 MeV Level
+ 4.030 MeV Level
+ 4.050 MeV Level
+ 4.070 MeV Level
+ 4.260 MeV Level
+ 4.290 MeV Level

| $\theta_{cm}$ deg. | $d\sigma/d\omega$ mb/str | $\Delta$ (%) + | $\Delta$ (%) − |
|---|---|---|---|
| 28.27 | 9.61 | 33.4 | 12.1 |
| 35.96 | 10.05 | 25.6 | 6.9 |
| 43.62 | 10.06 | 19.1 | 9.3 |
| 48.73 | 11.54 | 20.3 | 6.2 |
| 56.37 | 13.30 | 16.1 | 7.8 |
| 71.57 | 12.51 | 11.4 | 13.4 |
| 79.13 | 11.64 | 8.4 | 10.8 |
| 84.15 | 12.73 | 9.2 | 8.9 |
| 86.66 | 12.20 | 8.1 | 10.9 |
| 91.66 | 13.29 | 5.9 | 5.9 |
| 94.18 | 11.93 | 7.9 | 8.1 |
| 99.14 | 11.96 | 9.4 | 7.5 |
| 101.65 | 12.03 | 8.1 | 9.2 |
| 109.10 | 11.08 | 7.8 | 12.0 |
| 119.98 | 11.31 | 9.7 | 6.5 |
| 127.37 | 11.29 | 7.9 | 8.5 |
| 134.73 | 10.46 | 8.4 | 10.1 |

Avg. $d\sigma/d\omega$ = 11.68 mb/str ± 8.8 %
$\int(d\sigma/d\omega)d\omega$ = 146.78 mb ± 8.8 %

Data at the Following Angles
Excluded from the Average:
91.66

$E_n = 7.00 \pm 0.06$ MeV
(n,n') to: 4.030 MeV Level
+ 4.050 MeV Level
+ 4.070 MeV Level

| $\theta_{cm}$ deg. | $d\sigma/d\omega$ mb/str | $\Delta$ (%) + | $\Delta$ (%) − |
|---|---|---|---|
| 84.14 | 5.38 | 13.3 | 13.1 |
| 91.65 | 6.00 | 10.9 | 10.3 |
| 99.14 | 5.36 | 15.7 | 9.6 |

Avg. $d\sigma/d\omega$ = 5.67 mb/str ± 10.8 %
$\int(d\sigma/d\omega)d\omega$ = 71.25 mb ± 10.8 %

---

$E_n = 7.00 \pm 0.06$ MeV
(n,n') to: 4.260 MeV Level
+ 4.290 MeV Level

| $\theta_{cm}$ deg. | $d\sigma/d\omega$ mb/str | $\Delta$ (%) + | $\Delta$ (%) − |
|---|---|---|---|
| 84.22 | 3.82 | 18.7 | 16.9 |
| 91.72 | 3.99 | 17.9 | 19.9 |
| 99.20 | 3.33 | 21.1 | 18.1 |

Avg. $d\sigma/d\omega$ = 3.70 mb/str ± 13.7 %
$\int(d\sigma/d\omega)d\omega$ = 46.49 mb ± 13.7 %

---

$E_n = 7.50 \pm 0.03$ MeV
(n,n') to: 1.409 MeV Level

| $\theta_{cm}$ deg. | $d\sigma/d\omega$ mb/str | $\Delta$ (%) + | $\Delta$ (%) − |
|---|---|---|---|
| 83.68 | 5.74 | 21.6 | 15.1 |
| 91.18 | 4.41 | 18.1 | 8.8 |
| 98.67 | 3.07 | 45.5 | 11.4 |

$E_n = 7.50 \pm 0.03$ MeV
(n,n') to: 2.530 MeV Level

| $\theta_{cm}$ | $d\sigma/d\omega$ | $\Delta$ (%) | |
|---|---|---|---|
| *deg.* | *mb/str* | + | − |
| 83.81 | 3.06 | 18.0 | 15.5 |
| 91.32 | 2.71 | 22.9 | 10.8 |
| 98.80 | 2.20 | 29.7 | 25.3 |

Avg. $d\sigma/d\omega$ = 2.76 mb/str ± 14.2 %
$\int(d\sigma/d\omega)d\omega$ = 34.69 mb ± 14.2 %

---

$E_n = 7.50 \pm 0.03$ MeV
(n,n') to: 2.960 MeV Level
+ 3.160 MeV Level
+ 3.290 MeV Level
+ 3.340 MeV Level

| $\theta_{cm}$ | $d\sigma/d\omega$ | $\Delta$ (%) | |
|---|---|---|---|
| *deg.* | *mb/str* | + | − |
| 83.90 | 10.18 | 8.2 | 14.9 |
| 91.41 | 9.96 | 11.8 | 11.5 |
| 98.90 | 9.00 | 8.5 | 11.5 |

Avg. $d\sigma/d\omega$ = 9.38 mb/str ± 10.0 %
$\int(d\sigma/d\omega)d\omega$ = 117.82 mb ± 10.0 %

---

$E_n = 7.50 \pm 0.03$ MeV
(n,n') to: 3.840 MeV Level

| $\theta_{cm}$ | $d\sigma/d\omega$ | $\Delta$ (%) | |
|---|---|---|---|
| *deg.* | *mb/str* | + | − |
| 84.03 | 2.45 | 23.3 | 14.9 |
| 91.54 | 2.20 | 17.7 | 20.1 |
| 99.02 | 2.29 | 22.8 | 24.3 |

Avg. $d\sigma/d\omega$ = 2.32 mb/str ± 12.9 %
$\int(d\sigma/d\omega)d\omega$ = 29.20 mb ± 12.9 %

$E_n = 7.50 \pm 0.03$ MeV
(n,n') to: 3.840 MeV Level
+ 4.030 MeV Level
+ 4.050 MeV Level
+ 4.070 MeV Level
+ 4.260 MeV Level
+ 4.290 MeV Level

| $\theta_{cm}$ | $d\sigma/d\omega$ | $\Delta$ (%) | |
|---|---|---|---|
| *deg.* | *mb/str* | + | − |
| 84.08 | 9.48 | 10.8 | 12.6 |
| 91.59 | 9.91 | 7.5 | 14.0 |
| 99.08 | 8.75 | 11.7 | 14.8 |

Avg. $d\sigma/d\omega$ = 9.25 mb/str ± 10.8 %
$\int(d\sigma/d\omega)d\omega$ = 116.29 mb ± 10.8 %

---

$E_n = 7.50 \pm 0.03$ MeV
(n,n') to: 4.030 MeV Level
+ 4.050 MeV Level
+ 4.070 MeV Level

| $\theta_{cm}$ | $d\sigma/d\omega$ | $\Delta$ (%) | |
|---|---|---|---|
| *deg.* | *mb/str* | + | − |
| 84.08 | 4.30 | 14.5 | 14.0 |
| 91.59 | 4.47 | 19.4 | 13.3 |
| 99.07 | 3.65 | 18.3 | 12.9 |

Avg. $d\sigma/d\omega$ = 4.19 mb/str ± 11.6 %
$\int(d\sigma/d\omega)d\omega$ = 52.59 mb ± 11.6 %

---

$E_n = 7.50 \pm 0.03$ MeV
(n,n') to: 4.260 MeV Level
+ 4.290 MeV Level

| $\theta_{cm}$ | $d\sigma/d\omega$ | $\Delta$ (%) | |
|---|---|---|---|
| *deg.* | *mb/str* | + | − |
| 84.13 | 2.79 | 20.3 | 24.3 |
| 91.65 | 2.92 | 18.5 | 21.7 |
| 99.13 | 2.49 | 27.5 | 13.8 |

Avg. $d\sigma/d\omega$ = 2.75 mb/str ± 16.0 %
$\int(d\sigma/d\omega)d\omega$ = 34.51 mb ± 16.0 %

$E_n$ = 8.01 ± 0.03 MeV
(n,n') to: 1.409 MeV Level

| $\theta_{cm}$ | dσ/dω | Δ (%) | |
|---|---|---|---|
| *deg.* | *mb/str* | + | − |
| 83.67 | 4.54 | 12.6 | 11.5 |
| 91.18 | 4.77 | 15.2 | 14.8 |
| 98.67 | 4.23 | 19.3 | 12.5 |

---

$E_n$ = 8.01 ± 0.03 MeV
(n,n') to: 2.530 MeV Level

| $\theta_{cm}$ | dσ/dω | Δ (%) | |
|---|---|---|---|
| *deg.* | *mb/str* | + | − |
| 83.79 | 2.15 | 25.0 | 17.4 |
| 91.29 | 2.23 | 15.9 | 13.1 |
| 98.79 | 2.84 | 29.5 | 19.5 |

Avg. dσ/dω = 2.35 mb/str ± 13.6%
∫(dσ/dω)dω = 29.53 mb ± 13.6 %

---

$E_n$ = 8.01 ± 0.03 MeV
(n,n') to: 2.960 MeV Level
+ 3.160 MeV Level
+ 3.290 MeV Level
+ 3.340 MeV Level

| $\theta_{cm}$ | dσ/dω | Δ (%) | |
|---|---|---|---|
| *deg.* | *mb/str* | + | − |
| 83.87 | 7.77 | 14.6 | 10.0 |
| 91.38 | 8.27 | 11.7 | 8.6 |
| 98.87 | 7.69 | 15.2 | 21.0 |

Avg. dσ/dω = 8.06 mb/str ± 10.2%
∫(dσ/dω)dω = 101.34 mb ± 10.2 %

$E_n$ = 8.01 ± 0.03 MeV
(n,n') to: 3.840 MeV Level

| $\theta_{cm}$ | dσ/dω | Δ (%) | |
|---|---|---|---|
| *deg.* | *mb/str* | + | − |
| 83.98 | 2.03 | 20.3 | 11.9 |
| 91.49 | 2.25 | 16.5 | 19.0 |
| 98.98 | 2.53 | 15.4 | 19.9 |

Avg. dσ/dω = 2.24 mb/str ± 13.9%
∫(dσ/dω)dω = 28.12 mb ± 13.9 %

---

$E_n$ = 8.01 ± 0.03 MeV
(n,n') to: 3.840 MeV Level
+ 4.030 MeV Level
+ 4.050 MeV Level
+ 4.070 MeV Level
+ 4.260 MeV Level
+ 4.290 MeV Level

| $\theta_{cm}$ | dσ/dω | Δ (%) | |
|---|---|---|---|
| *deg.* | *mb/str* | + | − |
| 84.03 | 7.52 | 10.9 | 12.6 |
| 91.54 | 7.53 | 12.2 | 10.7 |
| 99.02 | 7.38 | 19.7 | 18.0 |

Avg. dσ/dω = 7.51 mb/str ± 10.8%
∫(dσ/dω)dω = 94.35 mb ± 10.8 %

---

$E_n$ = 8.01 ± 0.03 MeV
(n,n') to: 4.030 MeV Level
+ 4.050 MeV Level
+ 4.070 MeV Level

| $\theta_{cm}$ | dσ/dω | Δ (%) | |
|---|---|---|---|
| *deg.* | *mb/str* | + | − |
| 84.02 | 3.31 | 16.8 | 16.8 |
| 91.53 | 3.06 | 12.5 | 13.6 |
| 99.02 | 2.95 | 20.5 | 20.9 |

Avg. dσ/dω = 3.10 mb/str ± 11.9%
∫(dσ/dω)dω = 38.94 mb ± 11.9 %

$E_n = 8.01 \pm 0.03$ MeV
(n,n') to: 4.260 MeV Level
+ 4.290 MeV Level

| $\theta_{cm}$ | $d\sigma/d\omega$ | Δ (%) | |
|---|---|---|---|
| *deg.* | *mb/str* | + | − |
| 84.07 | 2.25 | 16.5 | 21.8 |
| 91.58 | 1.89 | 32.0 | 31.6 |
| 99.07 | 1.84 | 20.0 | 24.7 |

Avg. $d\sigma/d\omega =$ 1.97 mb/str ± 15.5 %
$\int(d\sigma/d\omega)d\omega =$ 24.76 mb ± 15.5 %

$E_n = 8.50 \pm 0.05$ MeV
Elastic Scattering

| $\theta_{cm}$ | $d\sigma/d\omega$ | Δ (%) | |
|---|---|---|---|
| *deg.* | *mb/str* | + | − |
| 13.10 | 2199.60 | 4.5 | 4.3 |
| 20.70 | 1611.44 | 4.7 | 4.4 |
| 27.99 | 851.12 | 4.8 | 4.7 |
| 28.30 | 969.11 | 5.9 | 5.9 |
| 35.61 | 441.18 | 4.7 | 5.0 |
| 43.22 | 158.95 | 6.0 | 6.1 |
| 48.29 | 65.02 | 7.5 | 7.6 |
| 55.87 | 12.27 | 20.8 | 18.0 |
| 63.45 | 1.72 | 97.2 | 91.6 |
| 71.01 | 6.98 | 23.5 | 23.2 |
| 78.54 | 13.00 | 12.9 | 14.5 |
| 83.56 | 14.51 | 12.5 | 12.9 |
| 86.06 | 14.11 | 13.7 | 12.5 |
| 91.06 | 17.27 | 15.6 | 13.3 |
| 93.56 | 15.53 | 11.0 | 10.7 |
| 98.56 | 15.49 | 19.3 | 11.9 |
| 101.05 | 16.38 | 9.9 | 11.5 |
| 108.52 | 12.36 | 16.3 | 14.8 |
| 119.44 | 7.42 | 16.3 | 16.1 |
| 126.86 | 3.79 | 32.7 | 29.4 |
| 134.28 | 3.15 | 44.8 | 42.5 |

$\int(d\sigma/d\omega)d\omega =$ 1831.70 mb ± 7.3 %
Wick's Limit = 2760.17 mb ± 9.2 %
$\sigma_T =$ 3.32 b ± 3.0 %

Legendre Fit, Order = 9

| *k* | $a_k$ | Δ(%) |
|---|---|---|
| 0 | 291.52466 | 2.0 |
| 1 | 251.84975 | 2.1 |
| 2 | 205.21701 | 2.3 |
| 3 | 157.05379 | 2.5 |
| 4 | 106.25903 | 3.0 |
| 5 | 61.10460 | 4.0 |
| 6 | 30.70152 | 5.9 |
| 7 | 13.14060 | 9.3 |
| 8 | 4.32615 | 17.5 |
| 9 | 0.90726 | 43.2 |

$E_n = 8.50 \pm 0.05$ MeV
(n,n′) to: 1.409 MeV Level

| $\theta_{cm}$ | $d\sigma/d\omega$ | Δ (%) | |
|---|---|---|---|
| *deg.* | *mb/str* | + | − |
| 35.67 | 8.84 | 47.9 | 16.7 |
| 43.29 | 6.71 | 18.7 | 17.4 |
| 48.36 | 4.96 | 49.0 | 17.4 |
| 55.96 | 4.35 | 20.4 | 9.5 |
| 63.54 | 4.38 | 11.0 | 11.0 |
| 71.10 | 4.88 | 17.5 | 12.3 |
| 78.65 | 5.10 | 21.5 | 12.2 |
| 83.66 | 5.60 | 14.3 | 13.8 |
| 86.16 | 4.62 | 13.3 | 11.2 |
| 91.17 | 4.41 | 19.2 | 18.4 |
| 98.66 | 3.48 | 23.3 | 27.6 |
| 101.16 | 4.05 | 21.0 | 15.4 |
| 108.61 | 4.04 | 23.7 | 18.9 |
| 119.53 | 4.73 | 15.6 | 15.4 |
| 126.95 | 4.60 | 17.2 | 13.2 |
| 134.35 | 3.92 | 29.2 | 11.1 |

$\int(d\sigma/d\omega)d\omega = 59.13$ mb ± 9.0 %

Legendre Fit, Order = 3

| *k* | $a_k$ | Δ(%) |
|---|---|---|
| 0 | 9.41119 | 5.7 |
| 1 | 0.68270 | 65.4 |
| 2 | 0.22804 | 130.0 |
| 3 | 0.19290 | 126.4 |

$E_n = 8.50 \pm 0.05$ MeV
(n,n′) to: 2.530 MeV Level

| $\theta_{cm}$ | $d\sigma/d\omega$ | Δ (%) | |
|---|---|---|---|
| *deg.* | *mb/str* | + | − |
| 43.45 | 2.56 | 18.5 | 21.0 |
| 56.05 | 1.67 | 27.2 | 21.4 |
| 71.21 | 1.99 | 26.7 | 24.1 |
| 83.77 | 2.64 | 18.2 | 20.3 |
| 86.27 | 1.93 | 18.4 | 26.3 |
| 91.28 | 2.02 | 17.5 | 19.7 |
| 93.78 | 1.67 | 19.2 | 24.8 |
| 98.77 | 2.20 | 18.5 | 27.7 |
| 101.26 | 2.02 | 22.5 | 29.3 |
| 108.73 | 1.09 | 31.6 | 35.5 |
| 119.63 | 1.63 | 19.3 | 20.2 |
| 127.04 | 1.17 | 50.2 | 32.6 |
| 134.43 | 2.04 | 20.5 | 26.8 |

Avg. $d\sigma/d\omega$ = 1.79 mb/str ± 10.7 %
$\int(d\sigma/d\omega)d\omega$ = 22.50 mb ± 10.7 %

---

$E_n = 8.50 \pm 0.05$ MeV
(n,n′) to: 2.960 MeV Level
+ 3.160 MeV Level
+ 3.290 MeV Level
+ 3.340 MeV Level

| $\theta_{cm}$ | $d\sigma/d\omega$ | Δ (%) | |
|---|---|---|---|
| *deg.* | *mb/str* | + | − |
| 48.50 | 6.95 | 14.6 | 21.9 |
| 56.11 | 6.23 | 12.9 | 19.2 |
| 63.71 | 6.03 | 9.6 | 18.0 |
| 71.28 | 5.20 | 10.5 | 19.2 |
| 83.84 | 7.40 | 9.2 | 17.3 |
| 86.35 | 6.67 | 9.9 | 26.1 |
| 91.34 | 6.48 | 10.7 | 17.4 |
| 93.85 | 6.79 | 10.8 | 14.4 |
| 98.84 | 6.79 | 12.2 | 17.9 |
| 101.34 | 5.55 | 13.0 | 19.2 |
| 108.79 | 6.39 | 11.7 | 23.0 |
| 119.69 | 5.46 | 13.7 | 16.5 |
| 127.10 | 5.65 | 17.2 | 8.4 |
| 134.48 | 5.85 | 11.2 | 12.2 |

Avg. $d\sigma/d\omega$ = 5.88 mb/str ± 9.2 %
$\int(d\sigma/d\omega)d\omega$ = 73.85 mb ± 9.2 %

$E_n$ = 8.50 ± 0.05 MeV
(n,n') to: 3.840 MeV Level
+ 4.030 MeV Level
+ 4.050 MeV Level
+ 4.070 MeV Level
+ 4.260 MeV Level
+ 4.290 MeV Level

| $\theta_{cm}$ | $d\sigma/d\omega$ | Δ (%) | |
|---|---|---|---|
| *deg.* | *mb/str* | + | − |
| 48.60 | 9.59 | 9.4 | 13.6 |
| 56.23 | 6.71 | 14.8 | 14.8 |
| 63.83 | 5.87 | 11.9 | 26.3 |
| 71.40 | 5.37 | 9.3 | 22.0 |
| 78.96 | 5.54 | 10.4 | 23.4 |
| 83.98 | 7.23 | 8.3 | 18.1 |
| 86.49 | 6.58 | 8.0 | 18.3 |
| 91.49 | 5.92 | 10.4 | 17.8 |
| 93.99 | 6.10 | 10.2 | 18.8 |
| 98.98 | 8.08 | 11.1 | 21.0 |
| 101.47 | 6.14 | 9.3 | 15.2 |
| 108.93 | 5.99 | 15.6 | 22.3 |
| 119.81 | 5.32 | 14.4 | 14.4 |
| 127.21 | 4.55 | 26.7 | 15.2 |
| 134.59 | 4.80 | 14.7 | 26.9 |

Avg. $d\sigma/d\omega$ = 5.66 mb/str ± 9.2 %
$\int(d\sigma/d\omega)d\omega$ = 71.08 mb ± 9.2 %

Data at the Following Angles
Excluded from the Average:
48.60

---

$E_n$ = 8.50 ± 0.05 MeV
(n,n') to: 3.840 MeV Level
+ 4.030 MeV Level
+ 4.050 MeV Level
+ 4.070 MeV Level
+ 4.260 MeV Level
+ 4.290 MeV Level
+ 4.580 MeV Level

| $\theta_{cm}$ | $d\sigma/d\omega$ | Δ (%) | |
|---|---|---|---|
| *deg.* | *mb/str* | + | − |
| 56.23 | 6.69 | 6.2 | 6.2 |

Avg. $d\sigma/d\omega$ = 6.69 mb/str ± 9.4 %
$\int(d\sigma/d\omega)d\omega$ = 84.03 mb ± 9.4 %